

1 **The long-term trend and production sensitivity change of the U.S. ozone pollution from**
2 **observations and model simulations**

3

4 Hao He^{1,2}, Xin-Zhong Liang^{1,2}, Chao Sun¹, Zhining Tao^{3,4}, and Daniel Q. Tong^{1,5}

5 ¹Department of Atmospheric and Oceanic Science, University of Maryland, College Park,
6 Maryland 20742, USA

7 ²Earth System Science Interdisciplinary Center, University of Maryland, College Park, Maryland
8 20740, USA

9 ³Universities Space Research Association, Columbia, Maryland 21046, USA

10 ⁴NASA Goddard Space Flight Center, Greenbelt, Maryland 20771, USA

11 ⁵Center for Spatial Information Science and Systems, George Mason University, Fairfax, VA
12 22030, USA

13

14 **Keywords:** Air Quality Trend, CMAQ Simulations, Ozone Production Sensitivity

15

16 Corresponding to Dr. Xin-Zhong Liang (xliang@umd.edu)

17

18 **Abstract**

19 We investigated the ozone pollution trend and its sensitivity to key precursors from 1990
20 to 2015 in the United States using long-term EPA AQS observations and mesoscale simulations.
21 The modeling system, a coupled regional climate – air quality (CWRF-CMAQ) model, well
22 captured summer surface ozone pollution during the past decades, having a mean slope of linear
23 regression with AQS observations at ~ 0.75 . While the AQS network has limited spatial coverage
24 and measures only a few key chemical species, the CWRF-CMAQ provides comprehensive
25 simulations to enable a more rigorous study of the change in ozone pollution and chemical
26 sensitivity. Analysis of seasonal variations and diurnal cycle of ozone observations showed that
27 peak ozone concentrations in the summer afternoon decreased ubiquitously across the United
28 States, up to 0.5 ppbv/yr in major non-attainment areas such as Los Angeles, while
29 concentrations at other hours such as the early morning and late afternoon increased slightly.
30 Consistent with the AQS observations, CMAQ simulated a similar decreasing trend of peak
31 ozone concentrations in the afternoon, up to 0.4 ppbv/yr, and increasing ozone trends in the early
32 morning and late afternoon. A monotonic decreasing trend (up to 0.5 ppbv/yr) in the odd oxygen
33 ($O_x = O_3 + NO_2$) concentrations are simulated by CMAQ at all daytime hours. This result
34 suggests that the increased ozone in the early morning and late afternoon was likely caused by
35 reduced NO-O₃ titration driven by continuous anthropogenic NO_x emission reductions in the past
36 decades. Furthermore, the CMAQ simulations revealed a shift in chemical regimes of ozone
37 photochemical production. From 1990 to 2015, surface ozone production in some metropolitan
38 areas, such as Baltimore, has transited from VOC-sensitive environment (>50% probability) to
39 NO_x-sensitive regime. Our results demonstrated that the long-term CWRF-CMAQ simulations
40 can provide detailed information of the ozone chemistry evolution under a changing climate, and

41 may partially explain the U.S. ozone pollution responses to regional and national regulations.

42

43 **1. Introduction**

44 Tropospheric ozone (O_3) is one of the major air pollutants, regulated by the U.S.
45 Environmental Protection Agency (EPA), that pose myriad threats to public health and the
46 environment (Adams et al., 1989; WHO, 2003; Ashmore, 2005; Anderson, 2009; Jerrett et al.,
47 2009). It is also an important greenhouse gas due to the absorption of thermal radiation, affecting
48 the climate (Fishman et al., 1979; Ramanathan and Dickinson, 1979; IPCC, 2013). The major
49 source of tropospheric ozone is photochemical production from ozone precursors such as carbon
50 monoxide (CO), volatile organic compounds (VOCs), and nitrogen oxides (NO_x) at the presence
51 of sunlight (Crutzen, 1974; Seinfeld, 1991; Jacob, 2000; EPA, 2006), while downward transport
52 of stratospheric air mass contributes substantially to ozone concentrations in upper troposphere
53 (Levy et al., 1985; Holton et al., 1995; Stevenson et al., 2006). In the past decades, ozone
54 pollution in the United States has been reduced substantially due to regulations on anthropogenic
55 emissions of ozone precursors (Oltmans et al., 2006; Lefohn et al., 2008, 2010; Cooper et al.,
56 2012; He et al., 2013; Cooper et al., 2014), although some studies suggested no trend or slight
57 increases at some rural areas (Jaffe and Ray, 2007; Lefohn et al., 2010; Cooper et al., 2012).
58 Most of these analyses focused on peak ozone concentrations, e.g., daily maximum 8-hour
59 average ozone (MDA8), during summer, but studies on trends in seasonal and diurnal patterns of
60 ozone pollution are limited. He et al. (2019) analyzed measurements from four monitoring sites
61 in the eastern United States and found different ozone trends between rural and urban sites from
62 the late 1990s to the early 2010s including some increases at certain hours, suggesting effects of
63 national regulations could be regionally dependent. Thus, it is important to extend our study to

64 other regions of the United States in a longer time period.

65 The non-monotonic trends in United States ozone pollution could be caused by the
66 complex non-linear chemistry of ozone production involving NO_x and VOCs (Logan et al., 1981;
67 Finlayson-Pitts and Pitts, 1999; Seinfeld and Pandis, 2006). With continuous reduction of
68 anthropogenic emissions of ozone precursors mainly NO_x and VOCs in the United States, we
69 need to better understand the photochemical regime change for local ozone production (i.e.,
70 ozone production sensitivity), because air pollution regulations could have different effects under
71 NO_x -sensitive and VOC-sensitive environment (Dodge, 1987; Kleinman, 1994). For instance,
72 under a VOC-sensitive photochemical regime, the decrease of NO_x emissions has limited
73 impacts on improving ozone pollution. Previous studies have developed photochemical
74 indicators to identify the ozone production sensitivity (Sillman, 1995; Sillman et al., 1997;
75 Tonnesen and Dennis, 2000b, 2000a; Sillman and He, 2002). Sillman (1999) found the ratio of
76 VOCs and NO_x (VOC/NO_x) has a typical value less than 4 for the VOC-sensitive environment
77 and higher than 15 for the NO_x -sensitive regime. Observation-based studies of ozone production
78 sensitivity relied on research grade measurements of ozone precursors and photochemical
79 intermediates that are not routinely measured by air quality management agencies such as the
80 U.S. EPA. These species include reactive nitrogen compounds (NO_y), nitric acid (HNO_3), and
81 hydrogen peroxide (H_2O_2), normally observed during field campaigns (e.g., Shon et al., 2007;
82 Peng et al., 2011) which only covered limited areas in certain periods. Studies based on air
83 quality models (AQM) could identify the ozone production regimes at regional scales (Sillman et
84 al., 1997; Sillman and He, 2002; Zhang et al., 2009a; Zhang et al., 2009b; Xie et al., 2011), but
85 the simulation periods were usually short (less than one year) and thus could not capture the
86 long-term change in ozone production sensitivity.

87 Regional AQMs are widely used for investigating the U.S. air quality (Tagaris et al.,
88 2007; Tang et al., 2009; Hogrefe et al., 2011; Pour-Biazar et al., 2011; He et al., 2016a; He et al.,
89 2018). They incorporate finer resolutions, more detailed emissions, and more explicit chemical
90 mechanism than global chemical transport models to better resolve characteristics of
91 tropospheric and surface dynamics, physical and chemical processes essential for air quality. Our
92 group has developed and used coupled regional climate-air quality models to study air quality
93 variations under a changing regional climate (Huang et al., 2007; Zhu and Liang, 2013; He et al.,
94 2016a; He et al., 2018). Our previous studies showed the model's ability to capture the decadal
95 U.S. air quality change (e.g., Zhu and Liang, 2013). In this study, we coupled the latest Climate-
96 Weather Research Forecast (CWRF) and the EPA Community Multiscale Air Quality (CMAQ)
97 models. CWRF has demonstrated substantial improvement in downscaling regional climate and
98 extremes (Liang et al., 2012; Chen et al., 2016; Liu et al., 2016; Liang et al., 2019; Sun and
99 Liang, 2020a; Sun and Liang, 2020b) and thus can provide more realistic weather conditions for
100 AQMs to produce more credible air quality simulations.

101 To supplement the limited observations in both spatial coverage and chemical species, we
102 conducted a continuous 26-yr CWRF-CMAQ simulation from 1990 to 2015 for a more rigorous
103 analysis of long-term U.S. ozone trend. The model performance of the U.S. air quality was first
104 evaluated against gridded ozone observations. The ozone seasonal variations and diurnal cycles
105 were then extracted to determine the observed long-term trend. The model simulations were
106 subsequently analyzed to explain the observed ozone trends and change in ozone production
107 sensitivity.

108 **2. Observations and model simulations**

109 **2.1 Long-term EPA observations**

110 Hourly measurements of surface ozone concentrations from 1990 to 2015 were available
111 from the EPA Air Quality System (AQS) database ([https://www.epa.gov/outdoor-air-quality-](https://www.epa.gov/outdoor-air-quality-data)
112 [data](https://www.epa.gov/outdoor-air-quality-data)). They have been examined following the EPA guidance including the quality assurance and
113 quality control. The locations and durations of AQS monitoring sites have changed substantially
114 due to logistics and requirements to cover the regions sensitive to air pollution. Figure 1 shows
115 that more than 2000 sites which reported ozone measurements during the period of 1990 to 2015.
116 To alleviate the impacts from missing data and short durations, we selected 640 sites that had
117 ozone observation records longer than 20 years. Hourly ozone observations were processed
118 following the approach described in He et al. (2019) to create the long-term seasonal and diurnal
119 records for these stations.

120

121 **2.2 Regional climate modeling**

122 CWRF (Liang et al., 2012) was driven by the European Centre for Medium-Range
123 Weather Forecasts ERA-Interim reanalysis (ERI, Dee et al., 2011) to downscale regional climate
124 variations during 1989-2015 with the first year as the spin-up and not used. We adopted the well-
125 established CWRF North American domain with a 30-km grid spacing (Fig. 1), covering the
126 Contiguous United States (CONUS) and neighboring southern Canada, northern Mexico and
127 adjacent oceans. The CWRF was developed as a climate extension of the WRF model
128 (Skamarock et al., 2008) incorporating numerous improvements in representation of physical
129 processes and integration of external forcings that are crucial to climate scales, including
130 interactions between land-atmosphere-ocean, convection-microphysics and cloud-aerosol-

131 radiation, and system consistency throughout all process modules (Liang et al., 2012; Qiao and
132 Liang, 2015; Chen et al., 2016; Liu et al., 2016; Qiao and Liang, 2016). CWRf is built with a
133 comprehensive ensemble of many alternate mainstream parameterization schemes for each of
134 key physical processes. . It has been vigorously tested in North America and Asia showing
135 outstanding performance to capture regional climate characteristics (Yuan and Liang, 2011; Chen
136 et al., 2016; Liu et al., 2016; Liang et al., 2019). The CWRf downscaling has been shown to
137 provide realistic meteorological fields and regional climate signals that can be cordially used to
138 drive the CMAQ for long air quality simulations. Major CWRf physics configurations include
139 the semi-empirical cloudiness parameterization of Xu and Randall (1996), the cloud
140 microphysics scheme of Tao et al. (1989), the short wave and long wave radiation scheme of
141 Chou et al. (2001), the ensemble cumulus parameterization (Qiao and Liang, 2015, 2016; Qiao
142 and Liang, 2017), and the planetary boundary layer scheme of Holtslag and Boville (1993).
143 Hourly CWRf outputs were processed using a modified Meteorology-Chemistry Interface
144 Processor (MCIP, version 4.3) for CMAQ simulations.

145

146 **2.3 Emissions preparation**

147 To prepare anthropogenic emissions, we chose 2014 as the baseline year. This year's
148 emissions were modified from the National Emissions Inventory 2011 (NEI2011). The
149 modifications were based on measurements from the Ozone Monitoring Instrument (OMI)
150 onboard satellite Aura, the ground-based AQS network, and the *in-situ* continuous emissions
151 monitoring in power plants (Tong et al., 2015; Tong et al., 2016). The so modified NEI2011
152 inventory was processed using the Sparse Matrix Operator Kernel Emissions (SMOKE) version
153 3.7 (Houyoux et al., 2000). Emissions from on-road, off-road, and area sources were placed at

154 the model layer closest to the surface. Emissions from point sources, e.g., stacks from power
155 plants, were distributed vertically based on stack height and plume rise. The plume rise was
156 estimated based on the method in Briggs (1972). The inventory pollutants were speciated
157 according to the carbon bond chemical mechanism version 5 (CB05) and AERO5 aerosol
158 mechanism. To fill the gap where NEI2011 data were not available, the Emissions Database for
159 Global Atmospheric Research (EDGAR v3, <http://edgar.jrc.ec.europa.eu/>) at a $1^\circ \times 1^\circ$ resolution
160 developed by the Joint Research Centre of European Commission was adapted. Figure 2 shows
161 an example of 2010-2015 mean NO_x emissions distribution over the modeling domain. Daily
162 mean NO_x emissions have high values in urban areas of cities such as Los Angeles, Chicago, and
163 the northeast corridor from Washington D.C. to Boston.

164 To project emissions from the baseline year into all individual years, we used the scaling
165 factors from Air Pollutant Emissions Trends (APET) data compiled by the U.S. EPA
166 (<https://www.epa.gov/air-emissions-inventories/air-pollutant-emissions-trends-data>). Emissions
167 of the baseline year are based on EPA NEI2011 inventory which can provide the best available
168 anthropogenic emissions to the CONUS and are currently used in the operational U.S. national
169 air quality forecast. The usage of APET scaling factors can guarantee the domain total emissions
170 are consistent with the U.S. EPA emissions trend, although assuming the same spatial
171 distribution of anthropogenic emissions from year to year may not be realistic. Without a
172 reasonable observation of actual spatiotemporal variations, it is the cost-effective approach as a
173 first-order approximation to simulate long-term U.S. air quality driven by consistent CONUS
174 total anthropogenic emissions that account interannual trends. Figure 3 shows the emission
175 evolution from 1990 to 2015. Since 1990 anthropogenic emissions of NO_x , CO, sulfur dioxide
176 (SO_2), and VOCs had steady decreasing trends, with SO_2 experiencing the largest reduction. On

177 the other hand, anthropogenic PM_{2.5} and NH₃ emissions stayed mostly flat since the early 2000s.

178 The wildfire emissions were based on the Global Fire Emissions Database, Version 4 with
179 small fires (GFEDv4s, Randerson et al., 2017; van der Werf et al., 2017). The 0.25° × 0.25°
180 degree resolution GFEDv4s data were projected onto the modeling domain and speciated into the
181 CB05 and AERO5 species. GFEDv4s had a monthly resolution from 1997 to 2000 and daily
182 resolution from 2000 onward. Figure 4 illustrates the fire emissions evolution during 1990 to
183 2015 relative to 2014. Fire emissions have large interannual variations, with high emissions in
184 1998, 2002, 2013, and 2015, and low emissions in 2001, 2004, and 2014. We developed a
185 method to merge the aforementioned anthropogenic and wildfire emissions into the
186 temporalized, gridded and speciated data ready for CMAQ.

187 The biogenic emissions were calculated on-line within CMAQ based on the Biogenic
188 Emissions Landuse Database, Version 3 (BELD3, [https://www.epa.gov/air-emissions-](https://www.epa.gov/air-emissions-modeling/biogenic-emissions-landuse-database-version-3-beld3)
189 [modeling/biogenic-emissions-landuse-database-version-3-beld3](https://www.epa.gov/air-emissions-modeling/biogenic-emissions-landuse-database-version-3-beld3)). The 1-km resolution BELD3
190 data with spatial distribution of 230 vegetation classes over the North America were processed
191 through the Spatial Allocator developed by the Community Modeling and Analysis System
192 (CMAS) center (<https://www.cmascenter.org/sa-tools/>) to generate the gridded vegetation
193 distribution over the study domain. Table 1 lists the 5-yr mean variations of daily major ozone
194 precursor (CO, NO_x, and NMVOCs) emissions in the modeling domain and five subdomains.
195 The emission data show regionally dependent reductions. For instance, compared with 2000-
196 2004, the NO_x emissions in 2005-2009 decreased by ~36% averaged in the CONUS, while 38%
197 and 35% reductions existed in states of California and Texas.

198 **2.4 Air quality modeling**

199 The EPA CMAQ model version 5.2 (EPA, 2017) was selected to simulate the U.S. air

200 quality variations driven by CWRM meteorological fields (Section 2.2) and constructed emissions
201 (Section 2.3). Major chemical mechanisms include the Carbon Bond 6 revision 3 (CB6r3) gas
202 phase chemical scheme with updated secondary organic aerosol (SOA) and nitrate chemistry
203 (Yarwood et al., 2010) and the latest AERO6 aerosol scheme (EPA, 2017), which improved U.S.
204 air quality simulations over previous chemical mechanisms (Appel et al., 2016). Chemical initial
205 and boundary conditions were obtained from the default concentration profiles built in CMAQ
206 (EPA, 2017). Simulations were conducted continuously for each 5-year segment (e.g., 1990-
207 1994, 1995-1999, etc.) with two-week spin-up in December prior to each starting years to speed
208 up simulation turn around. Hourly concentrations of ozone and its key precursors such as nitric
209 oxide (NO) and nitrogen dioxide (NO₂) were saved for subsequent analyses.

210

211 **3. Results**

212 **3.1 Evaluation of CMAQ performance**

213 Our previous studies showed that the direct comparison of observation data from
214 monitoring sites and CMAQ results in 30-km grid could introduce inconsistency for evaluating
215 the model performance (He et al., 2016a). The direct comparison is usually conducted through
216 sampling the grid of CMAQ where the AQS site is located, while the distribution of AQS
217 monitoring sites is usually uneven with more sites concentrated in populous urban and suburban
218 areas [where high ozone levels prevail](#). Sampling 30-km CMAQ grids over the locations of AQS
219 measurements, i.e. direct comparison of averaged concentrations in the 900 km² CMAQ grid and
220 pointwise AQS observations, could introduce important biases. So we applied the EPA Remote
221 Sensing Information Gateway (RSIG) software (available at <https://www.epa.gov/rsig>) to map
222 the site observations onto our CMAQ grid. The RISG has the capability to ‘re-grid’ the AQS

223 observations on a selected model grid using the inverse-distance-weighted method to calculate
224 the gridded mean concentrations (<https://www.epa.gov/hesc/how-rsig-regrids-data>). Figure 5
225 compares summer (JJA) mean MDA8 ozone in 2014 between gridded AQS observations and
226 CMAQ outputs and shows that the model can well capture the U.S. ozone pollution, except
227 underestimation in urban areas such as the Los Angeles basin.

228 Table 2 summarized the statistics of CMAQ performance simulating the summer ozone
229 concentrations during 2000 - 2015 in CONUS and subdomains. Linear regression analyses of
230 MDA8 ozone result in a mean slope value of 0.75 for CONUS, i.e., CMAQ slightly
231 underestimates ozone over the United States. In subdomains, CMAQ performance exhibits large
232 interannual variations. For instance, in Texas the linear regression slope and correlation
233 coefficient ranges from 0.58 to 0.97 and 0.55 to 0.86, respectively. With gradual reduction in
234 anthropogenic emissions, the fluctuations of CMAQ performance could be related to climate
235 signals which control the regional ozone pollution. Future work is needed to identify the
236 relationship between these regional climate variations and the U.S. ozone pollution. Generally,
237 this modeling system has substantially improved performance in the Southeast, California and
238 Texas, and moderately improved performance in the Northeast and Midwest as compared with
239 our previous modeling system (He et al., 2016a), which significantly underestimated the U.S.
240 ozone pollution. One reason is that CWRF with more sophisticated representation of physical
241 processes have the capability to better simulate the U.S. climate especially surface temperature
242 and precipitation (Liang et al., 2012; Chen et al., 2016; Liu et al., 2016; Sun and Liang, 2020a;
243 Sun and Liang, 2020b), which are key to accurate air quality simulations. The evaluation of
244 CMAQ performance demonstrates the capability of CWRF-CMAQ to credibly simulate
245 historical air quality.

246 **3.2 Long-term ozone trend in AQS observations**

247 We applied a box-averaging technique (He et al., 2016b; He et al., 2019) to analyze ozone
248 measurements at the selected AQS monitoring sites (Fig 1). This approach used an hour by
249 month box to calculate the mean 24-hr diurnal cycle of ozone for each month. Then we
250 calculated the climatology mean over 24 hours by 12 months and the respective anomaly for
251 each month at each AQS site. Figure 6 shows samples of long-term mean ozone concentrations
252 and anomalies at four non-attainment cities: Baltimore, Maryland; Los Angeles, California;
253 Denver, Colorado; and New York City (NYC), New York. The hour by month climatology (left
254 column of Fig. 6) shows that the peak ozone concentrations in the afternoon during the ozone
255 season (April to September) have been reduced significantly in these cities. However, ozone
256 concentrations in the morning (8 am to 12 pm, all local time hereafter) and at night (8 pm to 8
257 am) increased slightly. These results confirm the effectiveness of recent emission controls which
258 were designed to reduce the peak ozone. But the expansion of ozone at moderate levels (40-50
259 ppbv), which are higher than the natural background of U.S. ozone (Fiore et al., 2002; Fiore et
260 al., 2003; Wang et al., 2009; Lefohn et al., 2014), could cause negative health impacts.

261 The anomaly (right column of Fig. 6) shows large variabilities of ozone concentrations
262 because the ozone production is significantly impacted by regional climate (e.g., temperature,
263 precipitation) with interannual and decadal variations. Large ozone reduction occurred after 2003
264 when the EPA NO_x State Implementation (SIP) call was implemented (He et al., 2013). The
265 anomalies at Los Angeles (Fig. 6b) and NYC (Fig. 6d) shows decreases of the peak ozone in the
266 afternoon of summer and increases in other times and seasons. For Baltimore and Denver, the
267 peak ozone was not monotonically reduced, but increased in some years after 2002. Given the
268 continuous reduction of anthropogenic emissions in the past decades, the increased ozone

269 pollution in these areas could be caused by other factors, which need further investigations in the
270 future.

271 We used the linear regression analysis to calculate the slope, correlation (R), and p-value
272 of ozone trend at each local hour. Figure 7 shows ozone trends (slope, unit of ppbv/yr) at AQS
273 sites which are statistically significant ($R^2 > 0.5$, and $p < 0.05$) in the early morning (8 am), at
274 noon (12 pm), in the afternoon (4 pm), and in the evening (8 pm). Consistent results with the
275 four cities (Fig. 6) are found ubiquitously. The peak ozone at noon and in the afternoon generally
276 had a decreasing trend in CONUS, up to 0.5 ppbv/yr, confirming the improved air quality due to
277 regulations, while ozone in the early morning and late afternoon increased slightly at most of
278 monitoring sites. However, AQS sites in the Bay area (San Francisco, California) and Denver
279 had stronger positive trends in the day time. The possible explanations include the trans-pacific
280 transport of ozone and its precursors to the U.S. West Coast (Hudman et al., 2004; Huang et al.,
281 2010; Lin et al., 2012b) and stratosphere-troposphere exchange of ozone to high altitude region
282 (Langford et al., 2009; Lin et al., 2012a).

283

284 **3.3. Ozone trends derived from CMAQ simulations**

285 We applied the same box-averaging technique to hourly surface ozone simulations
286 in CONUS and conducted the linear regression analysis to estimate the ozone trend at each
287 model grid (Fig. 8). Compared with ozone trends derived from AQS observations (Fig. 7), the
288 CMAQ model successfully captured the spatial pattern and magnitude of change in ozone
289 pollution. For instance, at 4 pm LT, CMAQ simulated up to 0.4 ppbv/yr decrease in surface
290 ozone in the eastern United States and south region of California state. However, CMAQ
291 simulated statistically insignificant trends (white color in Fig. 8c) at 4 pm LT in the Bay area,

292 Los Angeles, and Denver where AQS observations showed increasing trends (Fig. 7c). The
293 discrepancy occurred because our model used the static chemical lateral conditions (LBCs) that
294 did not include the change of trans-Pacific transport of air pollutants, which were known to
295 elevate the background ozone in the West Coast. Also CMAQ does not contain stratospheric
296 chemistry and hence cannot account the contribution of downward transport of stratospheric
297 ozone to the high altitude region.

298 Consistent with trends derived from AQS observations, CMAQ also simulated increasing
299 ozone trends in the early morning (8 am LT, Fig. 8a) and late afternoon (8 pm LT, Fig 8d),
300 especially in urban regions such as Los Angeles and Chicago. He et al. (2019) found ozone
301 increases from observations at four sites in the eastern United States and a possible cause
302 suggested by the reduced NO-O₃ titration through examining the trend in odd oxygen ($O_x = O_3 +$
303 NO_2). Due to known interferences from nitrogen compounds such as NO_x and organic nitrates to
304 standard NO₂ measurements employed by EPA (Fehsenfeld et al., 1987; Dunlea et al., 2007;
305 Dickerson et al., 2019), the analysis of O_x required research grade NO₂ analyzer (e.g., photolytic
306 NO₂ conversion) which are not available in current AQS network. Thus, our simulations provide
307 a unique opportunity to expand such study to the whole CONUS.

308 Trends in O_x concentrations simulated by CMAQ at 8 am, 12 pm, 4 pm, and 8 pm show a
309 consistent decreasing trend over the modeling domain, up to 0.5 ppbv/yr reductions in the eastern
310 United States (Fig. 9). The result confirms our hypothesis that the reduced NO-O₃ titration
311 elevated surface ozone concentrations in the early morning and late afternoon when the
312 photochemical production of ozone is low or not active. Nowadays, the EPA ozone standard
313 focuses on peak ozone concentrations, i.e., MDA8 ozone which usually has maximum values at
314 noon or in the early afternoon, so the damage from additional ozone exposure from these

315 elevated ozone concentrations in the early morning and late afternoon is not considered under the
316 current environment policy. These increased ozone levels could offset the benefit from reduced
317 peak ozone in past decades, which needs further investigations to provide scientific evidence for
318 future policy decision.

319

320 **3.4 Change in photochemical regime**

321 With the continuous reduction of ozone precursor emissions, changes in the complex O₃-
322 NO_x-VOC chemistry are anticipated. We used the O₃/NO_y ratio as the indicator to study the
323 photochemical regime change in the U.S. surface ozone production. The usage of O₃/NO_y ratio
324 was first proposed by Sillman (Sillman, 1995; Sillman et al., 1997). Sillman et al. (Sillman et al.,
325 1997) conducted a case study of observations in urban areas (Atlanta, New York, and Los
326 Angeles) and modeling results from the Urban Airshed Model and suggested the threshold of 7
327 as the transition region from VOC-sensitive environment to NO_x-sensitive environment. Zhang
328 et al. (2009a; 2009b) expanded this method to the CONUS with 1-year observations and CMAQ
329 simulations (36-km spatial resolution) and suggested a threshold of 15 for ozone pollution at the
330 national scale. In this study, we did not have access to the long-term research grade NO_y
331 observations from the AQS network and did not conduct sensitivity experiments (due to
332 computational resource limit) with reduced NO_x emissions following Sillman et al. (1997), so we
333 have to reply on the O₃/NO_y threshold from literature. We conducted a simple evaluation of our
334 CMAQ results and found the threshold of 7 could be more proper for urban areas and the
335 threshold of 15 should be more applicable for our study of the whole United State (Figure S1 in
336 the supplementary material). Please note that the O₃/NO_y ratio could depend on the modeling
337 framework, so due to the similarity of our modeling system (30-km CMAQ) and the model used

338 in Zhang et al. (2009a; 2009b), our analysis suggest the similar threshold of 15.

339 The threshold of 15 proposed by Zhang et al. (2009b) was adopted to identify the VOC-
340 sensitive or NO_x -sensitive regime, i.e., $\text{O}_3/\text{NO}_y < 15$ indicating the VOC-sensitive regime. For
341 each local hour, we calculated the probability when O_3/NO_y is lower than 15 in every month.
342 Figure 10 shows the probability of VOC-sensitive regime at 2 pm in July of 1995, 2005, and
343 2015. Most regions dominated by the VOC-sensitive chemistry are urban or suburban where
344 anthropogenic NO_x emissions are relatively high as compared with anthropogenic and/or
345 biogenic VOCs emissions, such as the Los Angeles basin, the Northeast corridor (Washington
346 D.C.-Baltimore-Philadelphia-NYC), and the Chicago metropolitan area. Noting that these maps
347 are created based on ozone photochemical production simulated at the surface level, so the
348 distributions are slightly different from recent studies using satellite data (Duncan et al., 2010;
349 Jin et al., 2017; Ring et al., 2018).

350 We calculated the mean probability of VOC-sensitivity (2 pm in July) in a 3×3 CMAQ
351 grid in metropolitan areas of Baltimore, Los Angeles, and NYC from 1990 to 2015 (Fig. 11).
352 CMAQ simulations suggest the transition from VOC-sensitive regime to NO_x -sensitive regime in
353 these urban areas. There were interannual variabilities in the probability of VOC-sensitive
354 photochemistry in Baltimore (~50%) and NYC (~80%) in the 1990s and the early 2000s. After
355 the EPA 2003 NO_x SIP call, anthropogenic NO_x emissions decreased substantially leading to
356 reduced ozone pollution in the eastern United States (He et al., 2013), so the photochemical
357 production of surface ozone is expected to gradually become NO_x -sensitive. In 2015, ozone
358 photochemical production in Baltimore was dominated by NO_x emissions (only ~20%
359 probability of VOC-sensitive), while NYC had higher probability (>50%) of VOC-sensitive
360 chemistry. In Los Angeles, ozone chemistry slowly leaned to NO_x -sensitive, but until 2015 the

361 local ozone production was still controlled by VOCs emissions. In regions with VOC-sensitive
362 photochemistry in summer, reduction in NO_x emissions had a limited impact on the local rate of
363 ozone production until the photochemistry of ozone production became NO_x-sensitive. Our
364 analysis can partially explain the different responses of ozone pollution in major U.S. cities to
365 national air quality regulations during the past decades (Cooper et al., 2012) and can provide
366 some insights for future policy decision.

367

368 **4. Conclusions and Discussion**

369 EPA AQS observations in the United States from 1990 to 2015 were analyzed to study the
370 trend in surface ozone seasonal variations and diurnal cycles. We found that the peak ozone
371 concentrations in the afternoon decreased significantly, especially in major non-attainment
372 regions, but the concentrations in the early morning and late afternoon increased slightly.
373 Regional climate-air quality model captured the long-term records of U.S. ozone pollution and
374 suggested that the increased ozone was caused by reduced NO-O₃ titration due to the continuous
375 reduction of NO_x emissions. Model simulations also showed changes in ozone photochemical
376 regime. The U.S. urban/suburban areas generally transited from the VOC-sensitive regime in the
377 early 1990s to more NO_x-sensitive regime recently. But ozone production in some cities such as
378 NYC and Los Angeles are still substantially impacted by VOC emissions. The current national
379 and regional regulations focus on the MDA8 ozone concentrations mainly determined by the
380 peak ozone in the afternoon. Our study revealed the elevated ozone concentrations in the early
381 morning and late afternoon which must be considered for their impacts on public health. When
382 NO_x emissions are currently the main target of national and regional control measures, our study
383 suggested that regulations on anthropogenic VOCs emissions could be important in certain

384 regions. This study can improve our understanding about the effectiveness of regulations in the
385 past decades and will provide scientific evidence for future policy decision.

386 Ozone production is highly non-linear, so accurate emissions are essential to simulate its
387 long-term variations. Due to limited resources, we scaled the anthropogenic emissions from a
388 baseline year (2014) to the 1990s using factors derived from the national trend data to construct
389 consistent emissions for the CONUS with respect to the EPA data. This scaling cannot accurately
390 reflect the detailed regional-dependent regulations for individual state such as the 2012 Health
391 Air Act in Maryland (He et al., 2016b). Also, because the GFED data were only available after
392 1997, the contribution of wildfire emissions to ozone pollution was not included in model
393 simulations between 1990 to 1996. Thus, we anticipated some uncertainties in ozone simulations
394 in the early 1990s. Our model also has limitations to reproduce ozone records in high altitude
395 regions such as Denver because of lacking the stratospheric chemistry in CMAQ and missing the
396 effect of stratosphere-troposphere exchange to surface ozone. Lastly, due to limited resources,
397 our experiments used static chemical LBCs for CMAQ, which excluded the long-range transport
398 of air pollutants into the United States. So our current modeling system cannot take the historical
399 changes of air pollution outside the United State into account. That is, the effect of long-range
400 transport of air pollutants through model domain boundaries is presumed to be secondary to the
401 long-term trends over the United States. For some West Coast regions such as the state of
402 California, the trans-Pacific transport had been enhanced in the past decades and could play a
403 more important role in determining the local air quality. With these increased air pollutant
404 transported into the United States, our study may underestimate the impacts of domestic
405 emission reductions to U.S. ozone pollution, especially in the West Coast and the Southwest. To
406 accurate evaluate the contribution from trans-boundary emission, dynamic LBCs from a global

407 chemical transport model is needed in the future study.

408

409 **Author contribution**

410 H.H., X.L., and Z.T. designed the experiment; H.H. and C.S. developed the CWRP-CMAQ
411 system and performed the CWRP modeling; Z.T. and D.T. prepared the emission data; H.H.
412 conducted the CMAQ simulations; H.H., Z.T., and C.S. analyzed the data; H.H. prepared the
413 manuscript with contributions from all co-authors.

414

415 **Acknowledgments**

416 This work was supported by the U.S. Environmental Protection Agency under Assistance
417 Agreement No. RD-83587601. It has not been formally reviewed by EPA. The views expressed
418 in this document are solely those of the authors and do not necessarily reflect those of the
419 funding Agency. EPA does not endorse any products or commercial services mentioned in this
420 publication. We thank the support of University of Illinois at Urbana-Champaign
421 (UIUC)/USEPA award 20110150701. We thank the National Center for Supercomputing
422 Applications (NCSA) and the National Center for Atmospheric Research (NCAR) Computation
423 and Information System Laboratory for supercomputing support. We thank Dr. Plessel Todd for
424 the help on the RSIG software (<https://www.epa.gov/rsig>).

425

426 **References**

- 427 Adams, R. M., Glycer, J. D., Johnson, S. L., and McCarl, B. A.: A reassessment of the economic-effects of ozone on
428 United-States agriculture, *Japca-the Journal of the Air & Waste Management Association*, 39, 960-968,
429 1989.
- 430 Anderson, H. R.: Air pollution and mortality: A history, *Atmospheric Environment*, 43, 142-152,
431 10.1016/j.atmosenv.2008.09.026, 2009.
- 432 Appel, K. W., Napelenok, S. L., Hogrefe, C., Foley, K. M., Pouliot, G., Murphy, B. N., Luecken, D. J., and Heath,
433 N.: Evaluation of the Community Multiscale Air Quality (CMAQ) Model Version 5.2, 2016 CMAS
434 Conference, Chapel Hill, NC., 2016.
- 435 Ashmore, M. R.: Assessing the future global impacts of ozone on vegetation, *Plant Cell Environ.*, 28, 949-964,

436 10.1111/j.1365-3040.2005.01341.x, 2005.

437 Briggs, G. A.: Chimney plumes in neutral and stable surroundings**Shwartz and Tulin, *Atmospheric Environment*, 6,

438 19–35 (1971), *Atmospheric Environment* (1967), 6, 507-510, [https://doi.org/10.1016/0004-6981\(72\)90120-](https://doi.org/10.1016/0004-6981(72)90120-5)

439 5, 1972.

440 Chen, L. G., Liang, X. Z., DeWitt, D., Samel, A. N., and Wang, J. X. L.: Simulation of seasonal US precipitation and

441 temperature by the nested CWRP-ECHAM system, *Climate Dynamics*, 46, 879-896, 10.1007/s00382-015-

442 2619-9, 2016.

443 Chou, M.-D., Suarez, M. J., Liang, X.-Z., Yan, M. M.-H., and Cote, C.: A thermal infrared radiation

444 parameterization for atmospheric studies, 2001.

445 Cooper, O., Parrish, D., Ziemke, J., Balashov, N., Cupeiro, M., Galbally, I., Gilge, S., Horowitz, L., Jensen, N., and

446 Lamarque, J.-F.: Global distribution and trends of tropospheric ozone: An observation-based review,

447 *Elementa: Science of the Anthropocene*, 2, 000029, 2014.

448 Cooper, O. R., Gao, R. S., Tarasick, D., Leblanc, T., and Sweeney, C.: Long-term ozone trends at rural ozone

449 monitoring sites across the United States, 1990-2010, *Journal of Geophysical Research-Atmospheres*, 117,

450 D22307, 10.1029/2012jd018261, 2012.

451 Crutzen, P. J.: Photochemical reactions initiated by and influencing ozone in unpolluted tropospheric air, *Tellus*, 26,

452 47-57, 1974.

453 Dee, D. P., Uppala, S. M., Simmons, A. J., Berrisford, P., Poli, P., Kobayashi, S., Andrae, U., Balmaseda, M. A.,

454 Balsamo, G., Bauer, P., Bechtold, P., Beljaars, A. C. M., van de Berg, L., Bidlot, J., Bormann, N., Delsol,

455 C., Dragani, R., Fuentes, M., Geer, A. J., Haimberger, L., Healy, S. B., Hersbach, H., Hólm, E. V., Isaksen,

456 L., Kållberg, P., Köhler, M., Matricardi, M., McNally, A. P., Monge-Sanz, B. M., Morcrette, J. J., Park, B.

457 K., Peubey, C., de Rosnay, P., Tavolato, C., Thépaut, J. N., and Vitart, F.: The ERA-Interim reanalysis:

458 configuration and performance of the data assimilation system, *Q. J. R. Meteorol. Soc.*, 137, 553-597,

459 10.1002/qj.828, 2011.

460 Dickerson, R. R., Anderson, D. C., and Ren, X.: On the use of data from commercial NO_x analyzers for air pollution

461 studies, *Atmospheric Environment*, 214, 116873, <https://doi.org/10.1016/j.atmosenv.2019.116873>, 2019.

462 Dodge, M.: *Chemistry of Oxidant Formation: Implications for Designing Effective Control Strategies U.S.*

463 *Environmental Protection Agency, Washington, D.C. EPA/600/D-87/114 (NTIS PB87179990)*, 1987.

464 Duncan, B. N., Yoshida, Y., Olson, J. R., Sillman, S., Martin, R. V., Lamsal, L., Hu, Y. T., Pickering, K. E., Retscher,

465 C., Allen, D. J., and Crawford, J. H.: Application of OMI observations to a space-based indicator of NO_x

466 and VOC controls on surface ozone formation, *Atmospheric Environment*, 44, 2213-2223,

467 10.1016/j.atmosenv.2010.03.010, 2010.

468 Dunlea, E. J., Herndon, S. C., Nelson, D. D., Volkamer, R. M., San Martini, F., Sheehy, P. M., Zahniser, M. S.,

469 Shorter, J. H., Wormhoudt, J. C., Lamb, B. K., Allwine, E. J., Gaffney, J. S., Marley, N. A., Grutter, M.,

470 Marquez, C., Blanco, S., Cardenas, B., Retama, A., Villegas, C. R. R., Kolb, C. E., Molina, L. T., and

471 Molina, M. J.: Evaluation of nitrogen dioxide chemiluminescence monitors in a polluted urban

472 environment, *Atmospheric Chemistry and Physics*, 7, 2691-2704, 2007.

473 EPA: CMAQ (Version 5.2) Scientific Document, Zenodo. <http://doi.org/10.5281/zenodo.1167892>, 2017.

474 EPA, U. S.: Air quality criteria for ozone and related photochemical oxidants, *Environ. Prot. Agency*, , Research

475 Triangle Park, N.C., 2006.

476 Fehsenfeld, F. C., Dickerson, R. R., Hubler, G., Luke, W. T., Nunnermacker, L. J., Williams, E. J., Roberts, J. M.,

477 Calvert, J. G., Curran, C. M., Delany, A. C., Eubank, C. S., Fahey, D. W., Fried, A., Gandrud, B. W.,

478 Langford, A. O., Murphy, P. C., Norton, R. B., Pickering, K. E., and Ridley, B. A.: A ground-based

479 intercomparison of NO, NO_x, and NO_y measurement techniques, *Journal of Geophysical Research-*

480 *Atmospheres*, 92, 14710-14722, 1987.

481 Finlayson-Pitts, B. J., and Pitts, J. N.: *Chemistry of the Upper and Lower Atmosphere*, 1st ed., Academic Press, UK,

482 1999.

483 Fiore, A., Jacob, D. J., Liu, H., Yantosca, R. M., Fairlie, T. D., and Li, Q.: Variability in surface ozone background

484 over the United States: Implications for air quality policy, *Journal of Geophysical Research: Atmospheres*,

485 108, 10.1029/2003jd003855, 2003.

486 Fiore, A. M., Jacob, D. J., Bey, I., Yantosca, R. M., Field, B. D., Fusco, A. C., and Wilkinson, J. G.: Background

487 ozone over the United States in summer: Origin, trend, and contribution to pollution episodes, *Journal of*

488 *Geophysical Research: Atmospheres*, 107, ACH 11-11-ACH 11-25, 10.1029/2001jd000982, 2002.

489 Fishman, J., Ramanathan, V., Crutzen, P. J., and Liu, S. C.: Tropospheric ozone and climate, *Nature*, 282, 818-820,

490 10.1038/282818a0, 1979.

491 He, H., Stehr, J. W., Hains, J. C., Krask, D. J., Doddridge, B. G., Vinnikov, K. Y., Canty, T. P., Hosley, K. M.,

492 Salawitch, R. J., Worden, H. M., and Dickerson, R. R.: Trends in emissions and concentrations of air
493 pollutants in the lower troposphere in the Baltimore/Washington airshed from 1997 to 2011, *Atmospheric*
494 *Chemistry and Physics*, 13, 7859-7874, 10.5194/acp-13-7859-2013, 2013.

495 He, H., Liang, X.-Z., Lei, H., and Wuebbles, D. J.: Future U.S. ozone projections dependence on regional emissions,
496 climate change, long-range transport and differences in modeling design, *Atmospheric Environment*, 128,
497 124-133, <https://doi.org/10.1016/j.atmosenv.2015.12.064>, 2016a.

498 He, H., Vinnikov, K. Y., Li, C., Krotkov, N. A., Jongeward, A. R., Li, Z. Q., Stehr, J. W., Hains, J. C., and Dickerson,
499 R. R.: Response of SO₂ and particulate air pollution to local and regional emission controls: A case study in
500 Maryland, *Earth Future*, 4, 94-109, 10.1002/2015ef000330, 2016b.

501 He, H., Liang, X. Z., and Wuebbles, D. J.: Effects of emissions change, climate change and long-range transport on
502 regional modeling of future US particulate matter pollution and speciation, *Atmospheric Environment*, 179,
503 166-176, 10.1016/j.atmosenv.2018.02.020, 2018.

504 He, H., Vinnikov, K. Y., Krotkov, N. A., Edgerton, E. S., Schwab, J. J., and Dickerson, R. R.: Chemical climatology
505 of atmospheric pollutants in the eastern United States: Seasonal/diurnal cycles and contrast under
506 clear/cloudy conditions for remote sensing, *Atmospheric Environment*, 206, 85-107,
507 <https://doi.org/10.1016/j.atmosenv.2019.03.003>, 2019.

508 Hogrefe, C., Hao, W., Zalewsky, E. E., Ku, J. Y., Lynn, B., Rosenzweig, C., Schultz, M. G., Rast, S., Newchurch, M.
509 J., Wang, L., Kinney, P. L., and Sistla, G.: An analysis of long-term regional-scale ozone simulations over
510 the Northeastern United States: variability and trends, *Atmospheric Chemistry and Physics*, 11, 567-582,
511 10.5194/acp-11-567-2011, 2011.

512 Holton, J. R., Haynes, P. H., McIntyre, M. E., Douglass, A. R., Rood, R. B., and Pfister, L.: Stratosphere-troposphere
513 exchange, *Reviews of Geophysics*, 33, 403-439, 10.1029/95rg02097, 1995.

514 Holtstlag, A. A. M., and Boville, B. A.: Local Versus Nonlocal Boundary-Layer Diffusion in a Global Climate
515 Model, *Journal of Climate*, 6, 1825-1842, 10.1175/1520-0442(1993)006<1825:lvnbl>2.0.co;2, 1993.

516 Houyoux, M. R., Vukovich, J. M., Coats Jr., C. J., Wheeler, N. J. M., and Kasibhatla, P. S.: Emission inventory
517 development and processing for the Seasonal Model for Regional Air Quality (SMRAQ) project, *Journal of*
518 *Geophysical Research: Atmospheres*, 105, 9079-9090, 10.1029/1999jd900975, 2000.

519 Huang, H. C., Liang, X. Z., Kunkel, K. E., Caughey, M., and Williams, A.: Seasonal simulation of tropospheric
520 ozone over the midwestern and northeastern United States: An application of a coupled regional climate
521 and air quality modeling system, *J. Appl. Meteorol. Climatol.*, 46, 945-960, 10.1175/jam2521.1, 2007.

522 Huang, M., Carmichael, G., Adhikary, B., Spak, S., Kulkarni, S., Cheng, Y., Wei, C., Tang, Y., Parrish, D., and
523 Oltmans, S.: Impacts of transported background ozone on California air quality during the ARCTAS-CARB
524 period—a multi-scale modeling study, *Atmospheric Chemistry and Physics*, 10, 6947-6968, 2010.

525 Hudman, R., Jacob, D. J., Cooper, O., Evans, M., Heald, C., Park, R., Fehsenfeld, F., Flocke, F., Holloway, J., and
526 Hübler, G.: Ozone production in transpacific Asian pollution plumes and implications for ozone air quality
527 in California, *Journal of Geophysical Research: Atmospheres*, 109, 2004.

528 IPCC: Climate Change 2013: The Physical Science Basis., Contribution of Working Group I to the Fifth Assessment
529 Report (AR5) of the Intergovernmental Panel on Climate Change, 1535 pp.,
530 doi:10.1017/CBO9781107415324, 2013.

531 Jacob, D. J.: Heterogeneous chemistry and tropospheric ozone, *Atmospheric Environment*, 34, 2131-2159,
532 10.1016/s1352-2310(99)00462-8, 2000.

533 Jaffe, D., and Ray, J.: Increase in surface ozone at rural sites in the western US, *Atmospheric Environment*, 41,
534 5452-5463, 10.1016/j.atmosenv.2007.02.34, 2007.

535 Jerrett, M., Burnett, R. T., Pope, C. A., Ito, K., Thurston, G., Krewski, D., Shi, Y., Calle, E., and Thun, M.: Long-
536 Term Ozone Exposure and Mortality, *N. Engl. J. Med.*, 360, 1085-1095, 10.1056/NEJMoa0803894, 2009.

537 Jin, X., Fiore, A. M., Murray, L. T., Valin, L. C., Lamsal, L. N., Duncan, B., Folkert Boersma, K., De Smedt, I.,
538 Abad, G. G., Chance, K., and Tonnesen, G. S.: Evaluating a Space-Based Indicator of Surface Ozone-NOx-
539 VOC Sensitivity Over Midlatitude Source Regions and Application to Decadal Trends, *Journal of*
540 *Geophysical Research: Atmospheres*, 122, 439-410,461, doi:10.1002/2017JD026720, 2017.

541 Kleinman, L. I.: Low and high NO_x tropospheric photochemistry, *Journal of Geophysical Research-Atmospheres*,
542 99, 16831-16838, 10.1029/94jd01028, 1994.

543 Langford, A., Aikin, K., Eubank, C., and Williams, E.: Stratospheric contribution to high surface ozone in Colorado
544 during springtime, *Geophysical Research Letters*, 36, 2009.

545 Lefohn, A. S., Shadwick, D., and Oltmans, S. J.: Characterizing long-term changes in surface ozone levels in the
546 United States (1980-2005), *Atmospheric Environment*, 42, 8252-8262, 10.1016/j.atmosenv.2008.07.060,
547 2008.

548 Lefohn, A. S., Shadwick, D., and Oltmans, S. J.: Characterizing changes in surface ozone levels in metropolitan and
549 rural areas in the United States for 1980-2008 and 1994-2008, *Atmospheric Environment*, 44, 5199-5210,
550 10.1016/j.atmosenv.2010.08.049, 2010.

551 Lefohn, A. S., Emery, C., Shadwick, D., Wernli, H., Jung, J., and Oltmans, S. J.: Estimates of background surface
552 ozone concentrations in the United States based on model-derived source apportionment, *Atmospheric
553 Environment*, 84, 275-288, <https://doi.org/10.1016/j.atmosenv.2013.11.033>, 2014.

554 Levy, H., Mahlman, J. D., Moxim, W. J., and Liu, S. C.: Tropospheric ozone - the role of transport, *Journal of
555 Geophysical Research-Atmospheres*, 90, 3753-3772, 10.1029/JD090iD02p03753, 1985.

556 Liang, X.-Z., Xu, M., Yuan, X., Ling, T., Choi, H. I., Zhang, F., Chen, L., Liu, S., Su, S., Qiao, F., He, Y., Wang, J.
557 X. L., Kunkel, K. E., Gao, W., Joseph, E., Morris, V., Yu, T.-W., Dudhia, J., and Michalakes, J.: Regional
558 Climate-Weather Research and Forecasting Model, *Bulletin of the American Meteorological Society*, 93,
559 1363-1387, 10.1175/bams-d-11-00180.1, 2012.

560 Liang, X.-Z., Sun, C., Zheng, X., Dai, Y., Xu, M., Choi, H. I., Ling, T., Qiao, F., Kong, X., Bi, X., Song, L., and
561 Wang, F.: CWRf performance at downscaling China climate characteristics, *Climate Dynamics*, 52, 2159-
562 2184, 10.1007/s00382-018-4257-5, 2019.

563 Lin, M., Fiore, A. M., Cooper, O. R., Horowitz, L. W., Langford, A. O., Levy, H., Johnson, B. J., Naik, V., Oltmans,
564 S. J., and Senff, C. J.: Springtime high surface ozone events over the western United States: Quantifying
565 the role of stratospheric intrusions, *Journal of Geophysical Research: Atmospheres*, 117, 2012a.

566 Lin, M., Fiore, A. M., Horowitz, L. W., Cooper, O. R., Naik, V., Holloway, J., Johnson, B. J., Middlebrook, A. M.,
567 Oltmans, S. J., and Pollack, I. B.: Transport of Asian ozone pollution into surface air over the western
568 United States in spring, *Journal of Geophysical Research: Atmospheres*, 117, 2012b.

569 Liu, S., Wang, J. X. L., Liang, X.-Z., and Morris, V.: A hybrid approach to improving the skills of seasonal climate
570 outlook at the regional scale, *Climate Dynamics*, 46, 483-494, 10.1007/s00382-015-2594-1, 2016.

571 Logan, J. A., Prather, M. J., Wofsy, S. C., and McElroy, M. B.: Tropospheric chemistry - a global perspective,
572 *Journal of Geophysical Research-Oceans and Atmospheres*, 86, 7210-7254, 10.1029/JC086iC08p07210,
573 1981.

574 Oltmans, S. J., Lefohn, A. S., Harris, J. M., Galbally, I., Scheel, H. E., Bodeker, G., Brunke, E., Claude, H., Tarasick,
575 D., Johnson, B. J., Simmonds, P., Shadwick, D., Anlauf, K., Hayden, K., Schmidlin, F., Fujimoto, T., Akagi,
576 K., Meyer, C., Nichol, S., Davies, J., Redondas, A., and Cuevas, E.: Long-term changes in tropospheric
577 ozone, *Atmospheric Environment*, 40, 3156-3173, 10.1016/j.atmosenv.2006.01.029, 2006.

578 Peng, Y. P., Chen, K. S., Wang, H. K., and Lai, C. H.: In Situ Measurements of Hydrogen Peroxide, Nitric Acid and
579 Reactive Nitrogen to Assess the Ozone Sensitivity in Pingtung County, Taiwan, *Aerosol and Air Quality
580 Research*, 11, 59-69, 10.4209/aaqr.2010.10.0091, 2011.

581 Pour-Biazar, A., Khan, M., Wang, L. H., Park, Y. H., Newchurch, M., McNider, R. T., Liu, X., Byun, D. W., and
582 Cameron, R.: Utilization of satellite observation of ozone and aerosols in providing initial and boundary
583 condition for regional air quality studies, *Journal of Geophysical Research-Atmospheres*, 116, D18309,
584 10.1029/2010jd015200, 2011.

585 Qiao, F., and Liang, X.-Z.: Effects of cumulus parameterization closures on simulations of summer precipitation
586 over the continental United States, *Climate Dynamics*, 49, 225-247, 10.1007/s00382-016-3338-6, 2017.

587 Qiao, F. X., and Liang, X. Z.: Effects of cumulus parameterizations on predictions of summer flood in the Central
588 United States, *Climate Dynamics*, 45, 727-744, 10.1007/s00382-014-2301-7, 2015.

589 Qiao, F. X., and Liang, X. Z.: Effects of cumulus parameterization closures on simulations of summer precipitation
590 over the United States coastal oceans, *J. Adv. Model. Earth Syst.*, 8, 764-785, 10.1002/2015ms000621,
591 2016.

592 Ramanathan, V., and Dickinson, R. E.: Role of stratospheric ozone in the zonal and seasonal radiative energy-
593 balance of the Earth-troposphere system, *Journal of the Atmospheric Sciences*, 36, 1084-1104, 1979.

594 Randerson, J. T., Van Der Werf, G. R., Giglio, L., Collatz, G. J., and Kasibhatla, P. S.: Global Fire Emissions
595 Database, Version 4.1 (GFEDv4). ORNL Distributed Active Archive Center, 2017.

596 Ring, A. M., Canty, T. P., Anderson, D. C., Vinciguerra, T. P., He, H., Goldberg, D. L., Ehrman, S. H., Dickerson, R.
597 R., and Salawitch, R. J.: Evaluating commercial marine emissions and their role in air quality policy using
598 observations and the CMAQ model, *Atmospheric Environment*, 173, 96-107,
599 <https://doi.org/10.1016/j.atmosenv.2017.10.037>, 2018.

600 Seinfeld, J. H., and Pandis, S. N.: *Atmospheric Chemistry and Physics: From Air Pollution to Climate Change*, 2nd
601 ed., John Wiley & Sons, Inc., 2006.

602 Seinfeld, J. H. e. a.: *Rethinking the Ozone Problem in Urban and Regional Air Pollution*, National Academics Press,
603 Washington, DC, 1991.

604 Shon, Z.-H., Lee, G., Song, S.-K., Lee, M., Han, J., and Lee, D.: Characteristics of reactive nitrogen compounds and
605 other relevant trace gases in the atmosphere at urban and rural areas of Korea during May–June, 2004,
606 *Journal of Atmospheric Chemistry*, 58, 203–218, 10.1007/s10874-007-9088-4, 2007.

607 Sillman, S.: The use of NO_y, H₂O₂, and HNO₃ as indicators for ozone-NO_x-hydrocarbon sensitivity in urban
608 locations, *Journal of Geophysical Research-Atmospheres*, 100, 14175–14188, 10.1029/94jd02953, 1995.

609 Sillman, S., He, D., Cardelino, C., and Imhoff, R. E.: The Use of Photochemical Indicators to Evaluate Ozone-NO_x-
610 Hydrocarbon Sensitivity: Case Studies from Atlanta, New York, and Los Angeles, *J. Air Waste Manage.*
611 *Assoc.*, 47, 1030–1040, 10.1080/10962247.1997.11877500, 1997.

612 Sillman, S.: The relation between ozone, NO_x and hydrocarbons in urban and polluted rural environments,
613 *Atmospheric Environment*, 33, 1821–1845, 10.1016/s1352-2310(98)00345-8, 1999.

614 Sillman, S., and He, D.: Some theoretical results concerning O₃-NO_x-VOC chemistry and NO_x-VOC indicators,
615 *Journal of Geophysical Research: Atmospheres*, 107, ACH 26-21-ACH 26-15, 10.1029/2001jd001123,
616 2002.

617 Skamarock, W. C., Klemp, J. B., Dudhia, J., Gill, D. O., Barker, D. M., Duda, M. G., Huang, X.-Y., Wang, W., and
618 Powers, J. G.: A Description of the Advanced Research WRF Version 3, NCAR Technical Note,
619 NCAR/TN-475+STR, 113 pp, 2008.

620 Stevenson, D. S., Dentener, F. J., Schultz, M. G., Ellingsen, K., van Noije, T. P. C., Wild, O., Zeng, G., Amann, M.,
621 Atherton, C. S., Bell, N., Bergmann, D. J., Bey, I., Butler, T., Cofala, J., Collins, W. J., Derwent, R. G.,
622 Doherty, R. M., Drevet, J., Eskes, H. J., Fiore, A. M., Gauss, M., Hauglustaine, D. A., Horowitz, L. W.,
623 Isaksen, I. S. A., Krol, M. C., Lamarque, J. F., Lawrence, M. G., Montanaro, V., Muller, J. F., Pitari, G.,
624 Prather, M. J., Pyle, J. A., Rast, S., Rodriguez, J. M., Sanderson, M. G., Savage, N. H., Shindell, D. T.,
625 Strahan, S. E., Sudo, K., and Szopa, S.: Multimodel ensemble simulations of present-day and near-future
626 tropospheric ozone, *Journal of Geophysical Research-Atmospheres*, 111, D08301, 10.1029/2005jd006338,
627 2006.

628 Sun, C., and Liang, X. Z.: Improving U.S. extreme precipitation simulation: Dependence on cumulus
629 parameterization and underlying mechanism, *Climate Dynamics*, to be submitted, 2020a.

630 Sun, C., and Liang, X. Z.: Improving U.S. extreme precipitation simulation: Sensitivity to physics parameterizations,
631 *Climate Dynamics*, to be submitted, 2020b.

632 Tagaris, E., Manomaiphiboon, K., Liao, K.-J., Leung, L. R., Woo, J.-H., He, S., Amar, P., and Russell, A. G.:
633 Impacts of global climate change and emissions on regional ozone and fine particulate matter
634 concentrations over the United States, *Journal of Geophysical Research: Atmospheres*, 112,
635 doi:10.1029/2006JD008262, 2007.

636 Tang, Y., Lee, P., Tsidulko, M., Huang, H.-C., McQueen, J. T., DiMego, G. J., Emmons, L. K., Pierce, R. B.,
637 Thompson, A. M., Lin, H.-M., Kang, D., Tong, D., Yu, S., Mathur, R., Pleim, J. E., Otte, T. L., Pouliot, G.,
638 Young, J. O., Schere, K. L., Davidson, P. M., and Stajner, I.: The impact of chemical lateral boundary
639 conditions on CMAQ predictions of tropospheric ozone over the continental United States, *Environmental*
640 *Fluid Mechanics*, 9, 43–58, 10.1007/s10652-008-9092-5, 2009.

641 Tao, W.-K., Simpson, J., and McCumber, M.: An Ice-Water Saturation Adjustment, *Mon. Weather Rev.*, 117, 231–
642 235, 10.1175/1520-0493(1989)117<0231:aiwsa>2.0.co;2, 1989.

643 Tong, D., Pan, L., Chen, W., Lamsal, L., Lee, P., Tang, Y., Kim, H., Kondragunta, S., and Stajner, I.: Impact of the
644 2008 Global Recession on air quality over the United States: Implications for surface ozone levels from
645 changes in NO_x emissions, *Geophysical Research Letters*, 43, 9280–9288, 10.1002/2016gl069885, 2016.

646 Tong, D. Q., Lamsal, L., Pan, L., Ding, C., Kim, H., Lee, P., Chai, T. F., Pickering, K. E., and Stajner, I.: Long-term
647 NO_x trends over large cities in the United States during the great recession: Comparison of satellite
648 retrievals, ground observations, and emission inventories, *Atmospheric Environment*, 107, 70–84,
649 10.1016/j.atmosenv.2015.01.035, 2015.

650 Tonnesen, G. S., and Dennis, R. L.: Analysis of radical propagation efficiency to assess ozone sensitivity to
651 hydrocarbons and NO_x: 1. Local indicators of instantaneous odd oxygen production sensitivity, *Journal of*
652 *Geophysical Research: Atmospheres*, 105, 9213–9225, 10.1029/1999jd900371, 2000a.

653 Tonnesen, G. S., and Dennis, R. L.: Analysis of radical propagation efficiency to assess ozone sensitivity to
654 hydrocarbons and NO_x: 2. Long-lived species as indicators of ozone concentration sensitivity, *Journal of*
655 *Geophysical Research: Atmospheres*, 105, 9227–9241, 10.1029/1999jd900372, 2000b.

656 van der Werf, G. R., Randerson, J. T., Giglio, L., van Leeuwen, T. T., Chen, Y., Rogers, B. M., Mu, M. Q., van
657 Marle, M. J. E., Morton, D. C., Collatz, G. J., Yokelson, R. J., and Kasibhatla, P. S.: Global fire emissions
658 estimates during 1997–2016, *Earth Syst. Sci. Data*, 9, 697–720, 10.5194/essd-9-697-2017, 2017.

659 Wang, H., Jacob, D. J., Le Sager, P., Streets, D. G., Park, R. J., Gilliland, A. B., and van Donkelaar, A.: Surface

660 ozone background in the United States: Canadian and Mexican pollution influences, *Atmospheric*
661 *Environment*, 43, 1310-1319, <https://doi.org/10.1016/j.atmosenv.2008.11.036>, 2009.

662 WHO: Health aspects of air pollution with particulate matter, ozone and nitrogen dioxide, World Health
663 Organisation, Bonn., 2003.

664 Xie, Y., Elleman, R., Jobson, T., and Lamb, B.: Evaluation of O₃-NO_x-VOC sensitivities predicted with the CMAQ
665 photochemical model using Pacific Northwest 2001 field observations, *Journal of Geophysical Research:*
666 *Atmospheres*, 116, 10.1029/2011jd015801, 2011.

667 Xu, K.-M., and Randall, D. A.: A Semiempirical Cloudiness Parameterization for Use in Climate Models, *Journal of*
668 *the Atmospheric Sciences*, 53, 3084-3102, 10.1175/1520-0469(1996)053<3084:ascpfu>2.0.co;2, 1996.

669 Yarwood, G. S., Whitten, G. Z., Jung, J., Heo, G., and Allen, D.: Development, Evaluation and Testing of Version 6
670 of the Carbon Bond Chemical Mechanism (CB6),
671 [https://www.tceq.texas.gov/assets/public/implementation/air/am/contracts/reports/pm/5820784005FY1026-](https://www.tceq.texas.gov/assets/public/implementation/air/am/contracts/reports/pm/5820784005FY1026-20100922-enviro-cb6.pdf)
672 [20100922-enviro-cb6.pdf](https://www.tceq.texas.gov/assets/public/implementation/air/am/contracts/reports/pm/5820784005FY1026-20100922-enviro-cb6.pdf), 2010.

673 Yuan, X., and Liang, X. Z.: Improving cold season precipitation prediction by the nested CWRP-CFS system,
674 *Geophysical Research Letters*, 38, L02706, 10.1029/2010gl046104, 2011.

675 Zhang, Y., Vijayaraghavan, K., Wen, X. Y., Snell, H. E., and Jacobson, M. Z.: Probing into regional ozone and
676 particulate matter pollution in the United States: 1. A 1 year CMAQ simulation and evaluation using
677 surface and satellite data, *Journal of Geophysical Research-Atmospheres*, 114, 10.1029/2009jd011898,
678 2009a.

679 Zhang, Y., Wen, X. Y., Wang, K., Vijayaraghavan, K., and Jacobson, M. Z.: Probing into regional O₃ and particulate
680 matter pollution in the United States: 2. An examination of formation mechanisms through a process
681 analysis technique and sensitivity study, *Journal of Geophysical Research-Atmospheres*, 114,
682 10.1029/2009jd011900, 2009b.

683 Zhu, J. H., and Liang, X. Z.: Impacts of the Bermuda High on Regional Climate and Ozone over the United States,
684 *Journal of Climate*, 26, 1018-1032, 10.1175/jcli-d-12-00168.1, 2013.

685

686

687 **Tables and Figures**

688

689 **Table 1.** Summary of multiyear mean average of daily CO, NO_x, and NMVOCs emissions in the
 690 CONUS and five subdomains. (Unit: mol/km² per second) Please note that our California and
 691 Texas subdomains include more area than the states of California and Texas.
 692

CONUS				Southeast		
Year	CO	NO _x	NMVOCs	CO	NO _x	NMVOCs
1990-1994	32.9	1.24	0.94	47.2	1.43	1.03
1995-1999	26.2	1.18	0.76	37.4	1.36	0.85
2000-2004	18.9	1.26	0.69	26.4	1.46	0.72
2005-2009	12.3	0.94	0.60	16.9	1.07	0.59
2010-2015	8.0	0.60	0.46	11.0	0.66	0.45
California				Northeast		
1990-1994	18.3	1.22	0.57	110.3	3.29	2.12
1995-1999	14.6	1.16	0.46	87.2	3.16	1.68
2000-2004	10.6	1.23	0.40	62.1	3.41	1.43
2005-2009	7.1	0.91	0.35	40.3	2.56	1.25
2010-2015	4.6	0.56	0.26	25.9	1.62	0.93
Texas				Midwest		
1990-1994	22.6	1.21	1.26	58.2	1.88	1.41
1995-1999	18.1	1.15	1.03	46.3	1.80	1.14
2000-2004	13.0	1.20	1.01	33.4	1.92	0.98
2005-2009	8.4	0.91	0.92	22.0	1.44	0.85
2010-2015	5.5	0.60	0.73	14.3	0.91	0.63

693

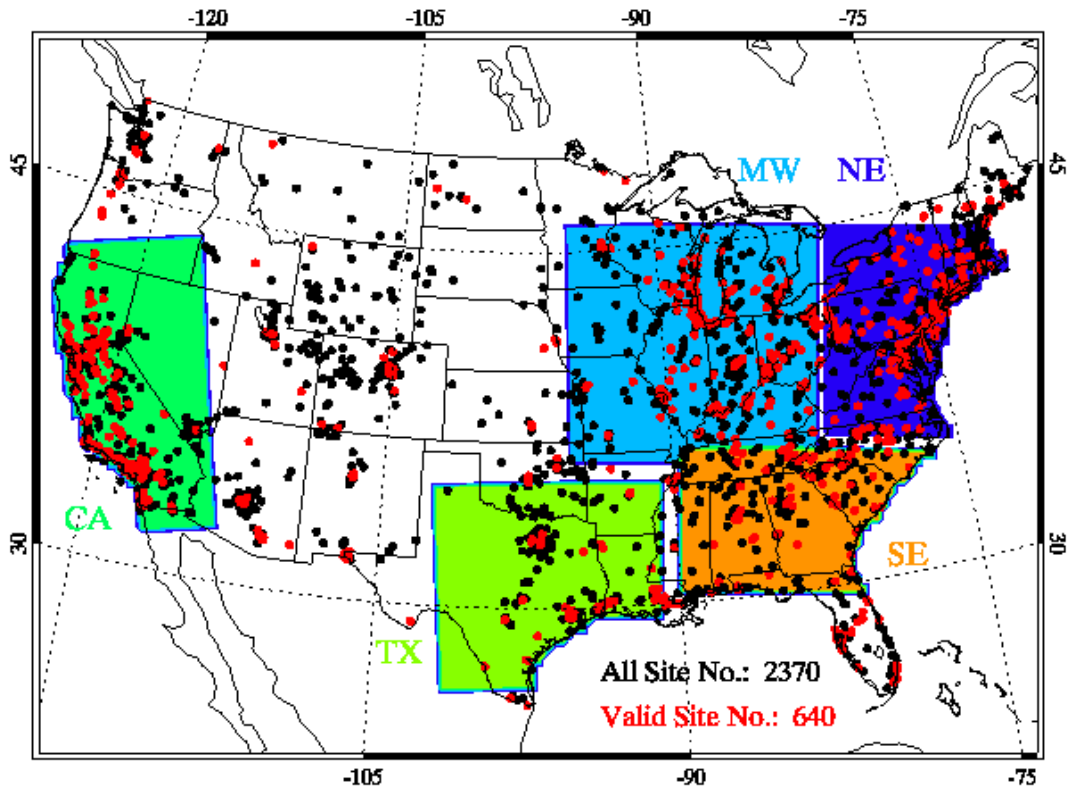
694 **Table 2.** Summary about the comparison of JJA MDA8 ozone concentrations from AQS
695 observations and CMAQ simulations during 2000-2015 in the CONUS and subdomains. Slope
696 and Correlation (Corr. R) are calculated for each year based on linear regression analysis. Please
697 note that our California and Texas subdomains include more area than the states of California
698 and Texas.
699

Year	Slope	Corr. R	NMB	RMSE	Year	Slope	Corr. R	NMB	RMSE
CONUS									
2000	0.73	0.37	-6.9	10.5	2008	0.70	0.54	-5.4	8.4
2001	0.80	0.61	-7.7	8.7	2009	0.78	0.35	-1.6	8.5
2002	0.71	0.63	-8.6	9.2	2010	0.75	0.51	-6.2	8.4
2003	0.81	0.60	-4.3	8.4	2011	0.77	0.42	-7.1	9.2
2004	0.85	0.39	1.3	8.9	2012	0.67	0.60	-10.7	9.3
2005	0.87	0.54	-7.3	8.8	2013	0.70	0.50	-1.8	7.9
2006	0.77	0.48	-7.6	9.1	2014	0.72	0.44	-3.0	7.6
2007	0.70	0.60	-6.1	8.0	2015	0.73	0.41	-4.2	7.7
California									
2000	0.70	0.67	-19.3	15.2	2008	0.63	0.53	-18.0	14.8
2001	0.72	0.63	-18.1	14.8	2009	0.67	0.61	-19.0	13.5
2002	0.80	0.55	-15.5	14.4	2010	0.62	0.55	-19.0	14.1
2003	0.80	0.55	-20.1	16.2	2011	0.68	0.57	-17.0	13.3
2004	0.78	0.51	-19.2	16.1	2012	0.64	0.63	-21.4	14.9
2005	0.78	0.54	-19.0	15.3	2013	0.64	0.60	-17.9	13.5
2006	0.80	0.61	-20.5	15.6	2014	0.69	0.56	-21.9	14.8
2007	0.69	0.65	-16.0	12.9	2015	0.72	0.61	-22.3	14.2
Texas									
2000	0.60	0.77	-20.4	11.8	2008	0.62	0.74	-10.5	6.6
2001	0.58	0.62	-19.6	11.5	2009	0.73	0.78	-17.1	8.7
2002	0.70	0.72	-10.4	6.6	2010	0.65	0.77	-9.4	5.3
2003	0.64	0.78	-8.8	6.5	2011	0.52	0.83	-22.7	12.1
2004	0.97	0.55	-7.2	5.8	2012	0.53	0.86	-17.8	9.4
2005	0.70	0.78	-21.5	11.4	2013	0.53	0.74	-11.6	6.9
2006	0.66	0.83	-20.5	11.3	2014	0.66	0.72	-5.0	4.7
2007	0.77	0.84	-4.0	3.9	2015	0.76	0.61	-10.1	5.8
Southeast									
2000	0.61	0.41	-20.5	13.3	2008	0.52	0.77	-13.4	8.3
2001	0.64	0.70	-7.7	6.2	2009	0.88	0.52	-2.7	4.2

2002	0.56	0.77	-14.1	9.5	2010	0.69	0.75	-7.8	5.1
2003	0.65	0.77	-0.7	4.7	2011	0.84	0.62	-13.5	8.2
2004	0.81	0.59	3.2	4.4	2012	0.62	0.73	-9.4	6.1
2005	0.54	0.64	-8.8	6	2013	0.74	0.70	7.0	4.1
2006	0.74	0.60	-14	9	2014	0.84	0.40	0.9	4.0
2007	0.56	0.71	-14.1	9	2015	0.71	0.44	-2.6	4.2
Northeast									
2000	0.50	0.25	7.9	7.0	2008	0.46	0.11	-0.5	5.8
2001	0.46	0.28	-3.6	6.0	2009	0.67	0.23	13.7	7.3
2002	0.51	0.13	-8.5	8.3	2010	0.49	0.10	-0.4	5.6
2003	0.85	0.16	3.0	5.3	2011	0.47	0.31	3.2	5.9
2004	0.81	0.21	10.0	6.6	2012	0.55	0.17	-2.9	5.3
2005	0.84	0.11	2.5	5.8	2013	0.78	0.45	11.6	6.4
2006	0.45	0.21	3.0	6.0	2014	0.60	0.33	-4.8	5.1
2007	0.48	0.19	-0.7	5.6	2015	0.49	0.11	2.2	5.1
Midwest									
2000	0.41	0.25	3.4	5.9	2008	0.44	0.25	3.5	4.7
2001	0.55	0.30	-2.3	4.9	2009	0.54	0.22	14	7.2
2002	0.45	0.27	-5.2	7.0	2010	0.57	0.12	2.4	5.3
2003	0.66	0.25	-0.1	4.7	2011	0.45	0.21	1.1	5.6
2004	0.68	0.44	13.9	7.5	2012	0.46	0.19	-11.6	8.3
2005	0.76	0.15	-4.4	5.6	2013	0.74	0.18	4.9	4.0
2006	0.50	0.17	0.3	5.0	2014	0.64	0.20	5.7	4.1
2007	0.39	0.20	-0.6	5.6	2015	0.68	0.27	8.7	4.7

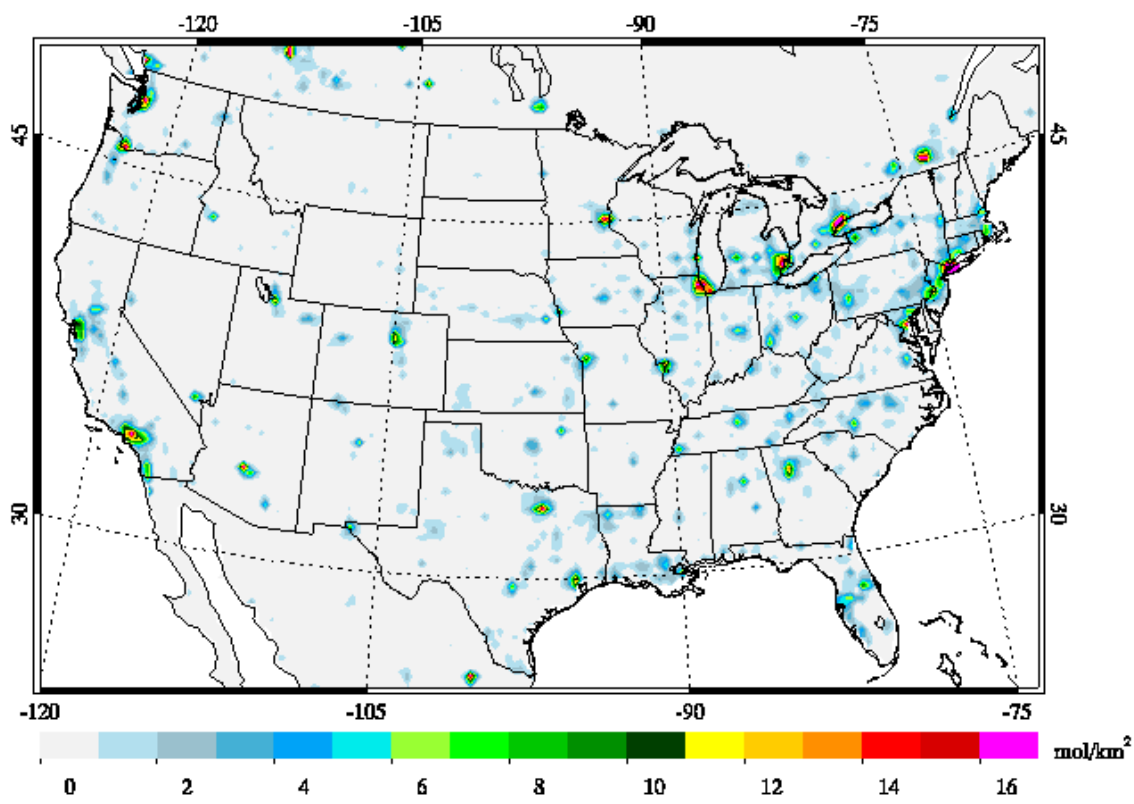
700 NMB: Normalized Mean Bias (Unit: %)
701 RMSE: Root Mean Square Error (Unit: ppbv)
702

703 **Figure 1.** Locations of EPA AQS sites for surface ozone monitoring during 1990-2015. Red dots
704 stand for monitoring sites with more than 20 year record. Black dots show the locations of
705 monitoring sites have short data records which are not used in this study. The map shows the
706 CWRf-CMAQ 30-km domain and five subdomains sensitive to air pollution. CA: California
707 (including nearby parts of Nevada, Arizona and Oregon); TX: Texas (including nearby parts of
708 Louisiana, Arkansas, and Oklahoma); SE: Southeast; NE: Northeast; MW: Midwest. Please note
709 that our CA and TX subdomains include more area than the states of California and Texas.



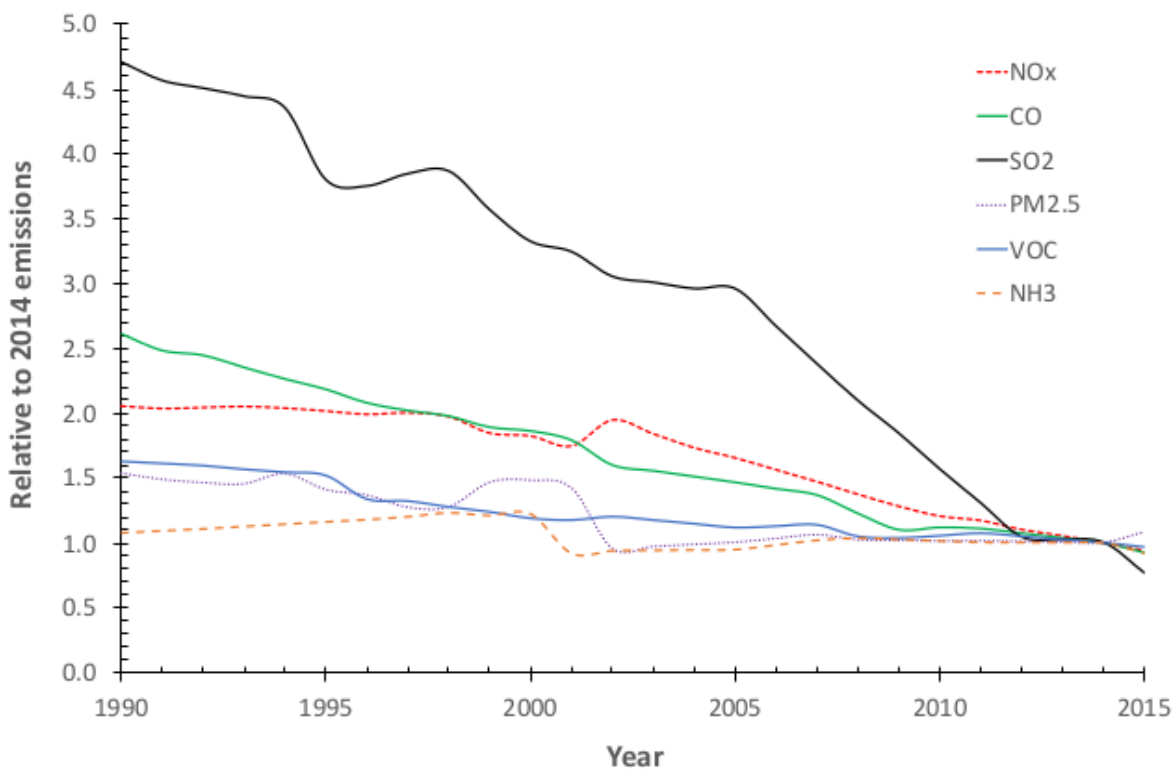
710

711 **Figure 2.** Averaged daily NO_x emissions between 2010 and 2015 in the modeling domain (Unit:
712 mol/km² per second).



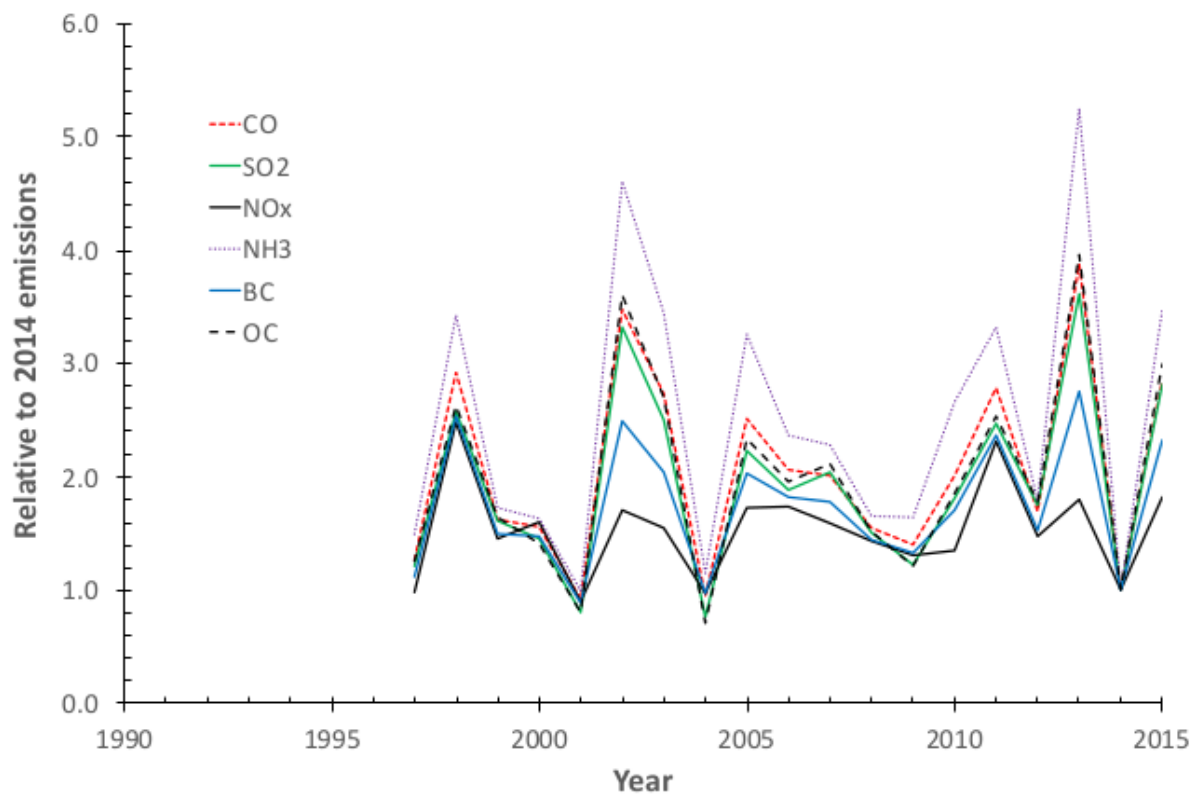
713

714 **Figure 3.** Anthropogenic emission evolution relative to 2014 in the modeling domain from 1990
715 – 2015.



716
717

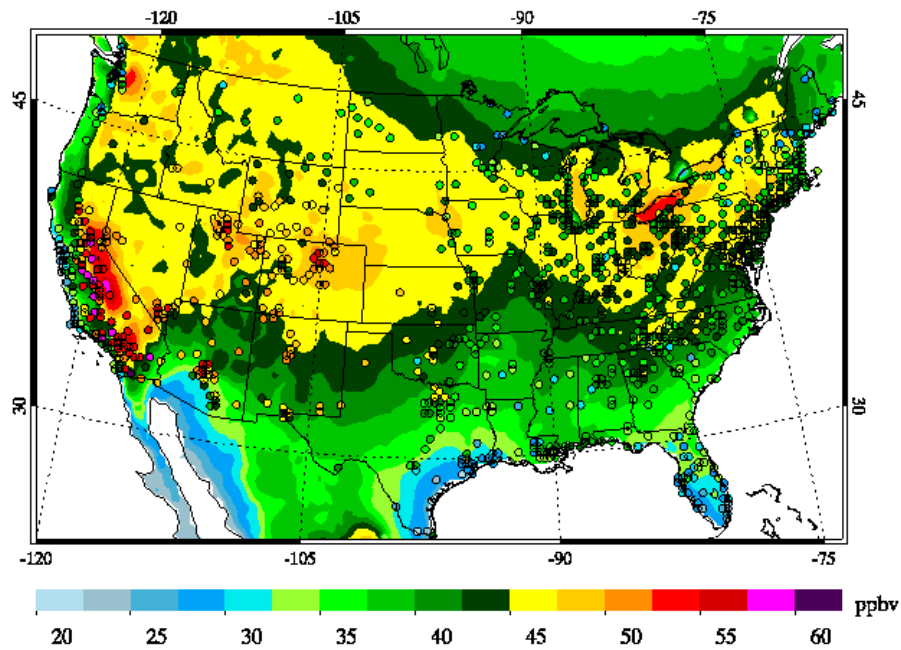
718 **Figure 4.** Fire emission evolution relative to 2014 in the modeling domain from 1990 – 2015.
719 Noting that GFED fire emissions are not available before 1997.



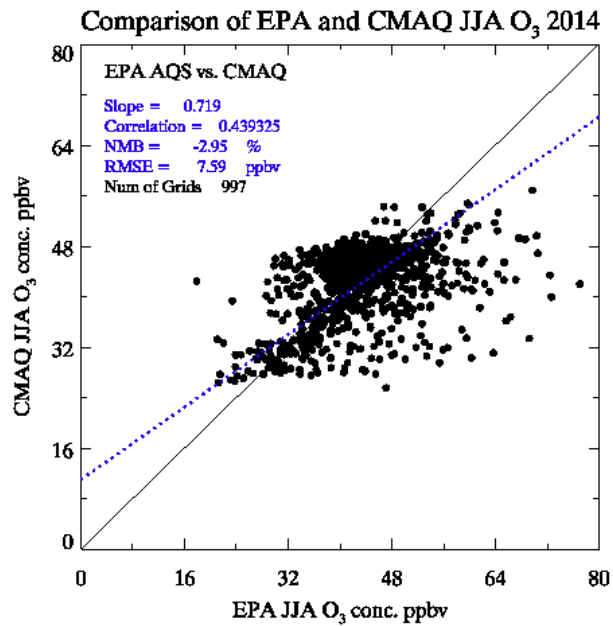
720

721 **Figure 5.** Comparison of summer MDA8 ozone concentrations from EPA AQS observations and
 722 CMAQ simulations in 2014. AQS station data were gridded to the CMAQ grid using the EPA
 723 RSIG software. a) Contour plot, the background stands for the CMAQ outputs and the dots stand
 724 for gridded AQS observations; b) Scatter plot of the gridded AQS observations and co-located
 725 CMAQ outputs.

726 a)

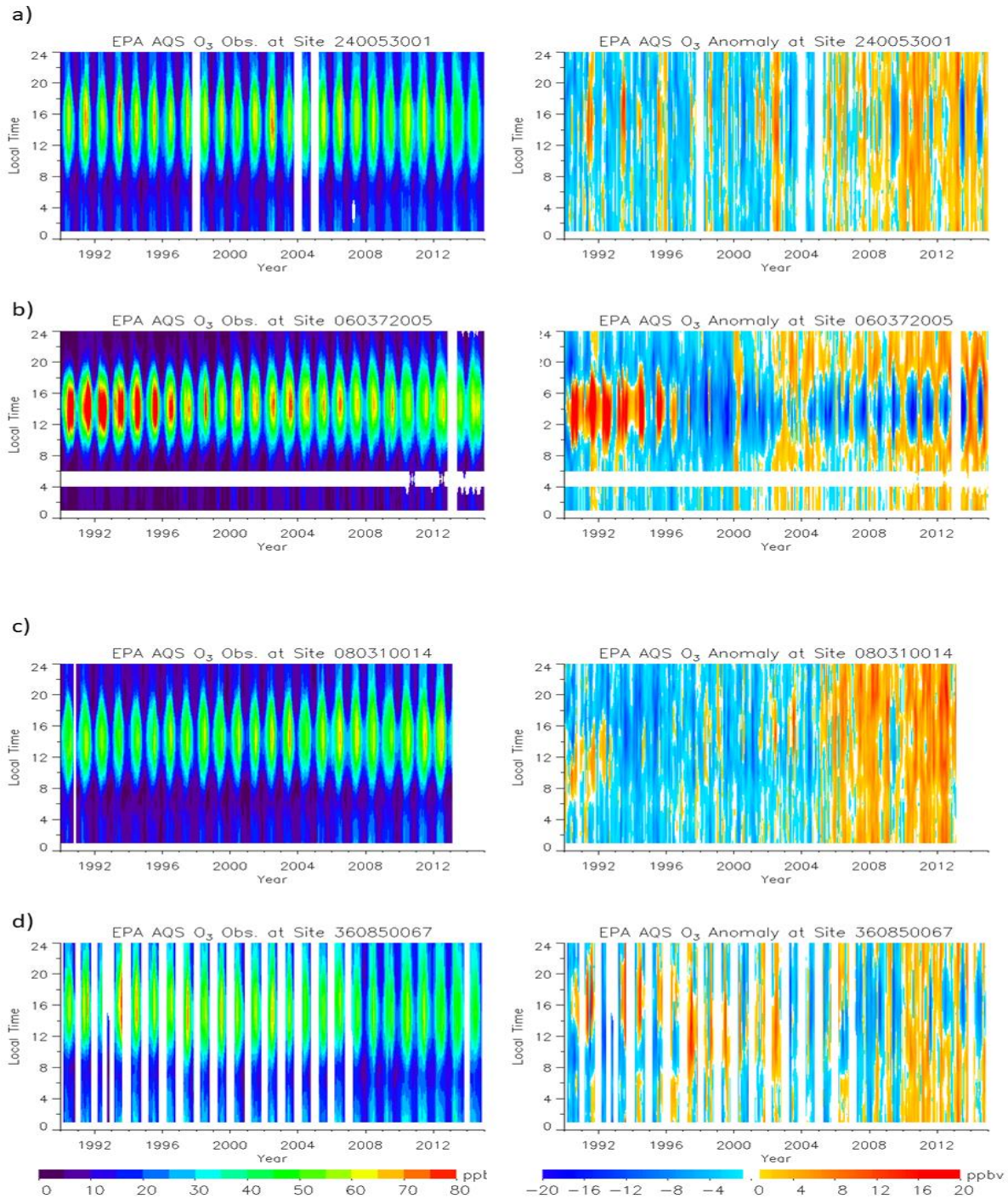


727
 728 b)



729

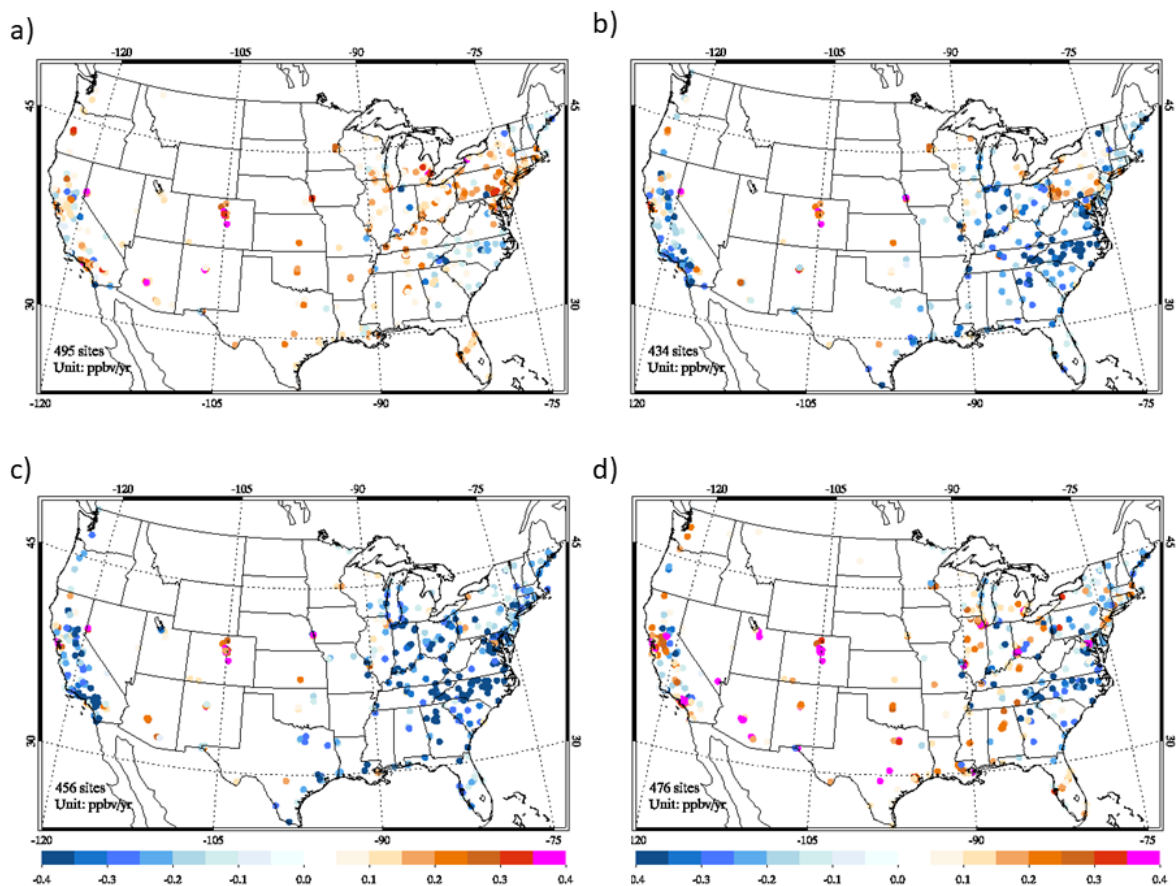
730 **Figure 6.** The box-averaging analyses of AQS ozone observations at selected sites from 1990-
 731 2015. a) Essex, Maryland (suburban Baltimore, AQS ID 240053001); b) Pasadena, California
 732 (downtown Los Angeles, AQS ID 060372005); c) Denver, Colorado (downtown Denver, AQS ID
 733 080310014); d) Staten Island, New York (suburban New York City, AQS ID: 360850067). Left
 734 column shows the monthly mean, right column shows the anomaly values. White patches stand
 735 for missing data or not sufficient data for the box-averaging analysis.



736

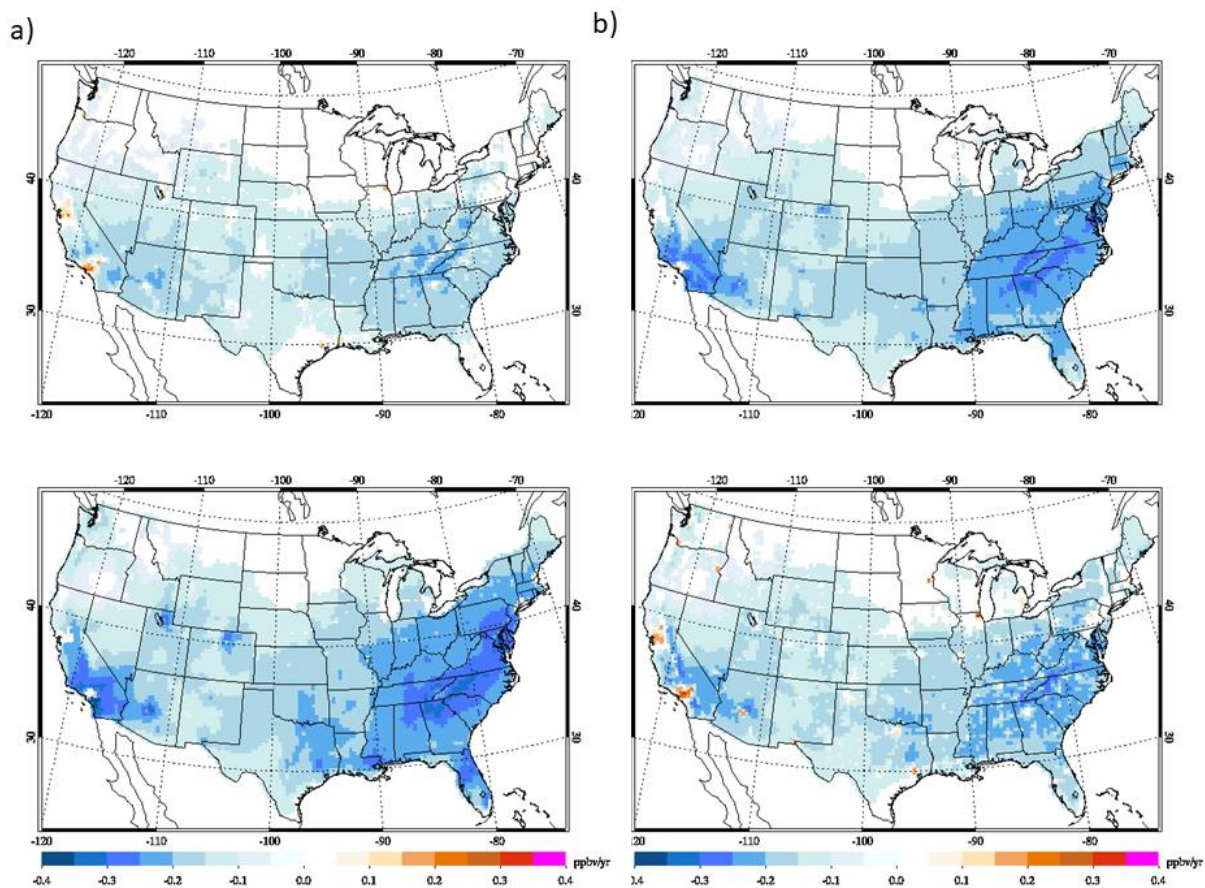
737

738 **Figure 7.** Trend in ozone observations at selected EPA AQS sites during 1990-2015 (Unit:
739 ppbv/yr). a) at 8 am; b) at 12 pm; c) at 4 pm; d) at 8 pm (all local time). We only show the sites
740 with statistically significant linear trend in the plots.



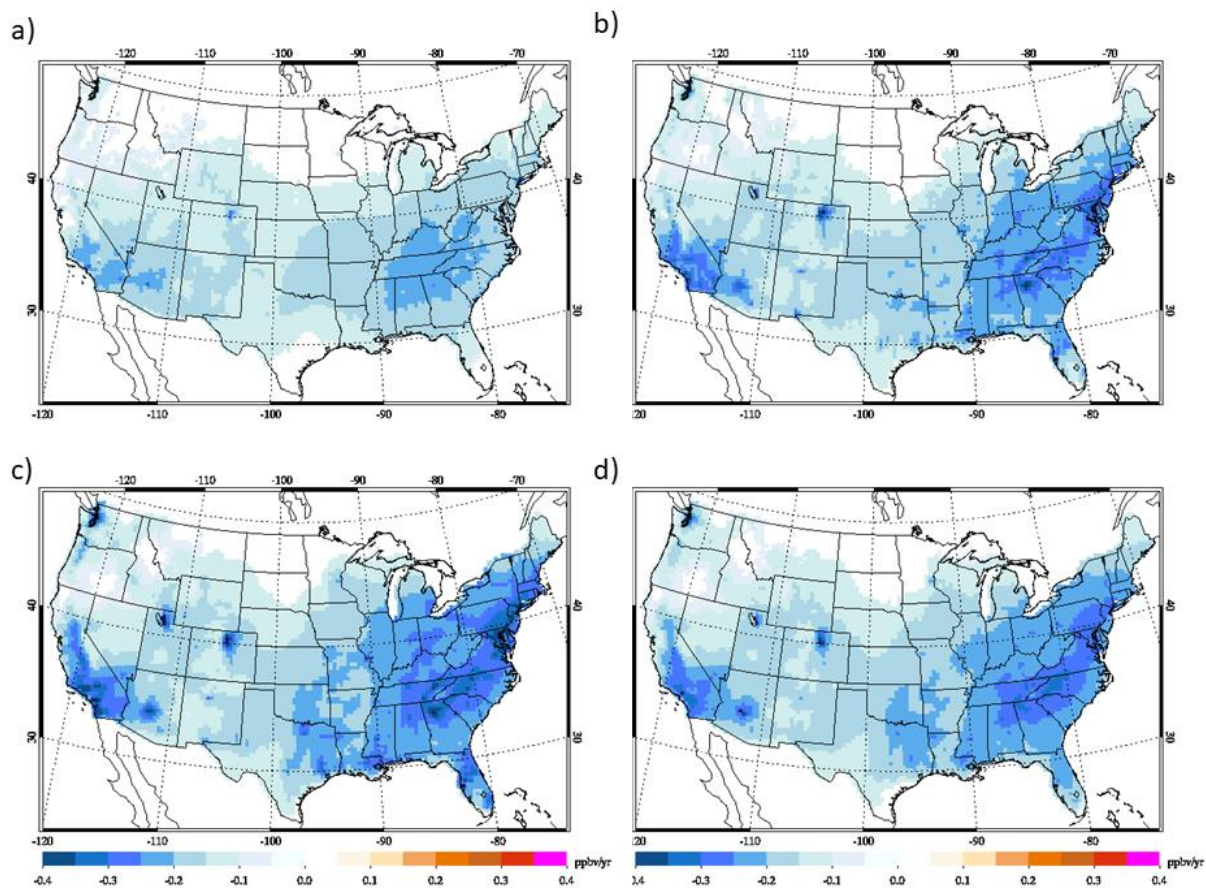
741

742 **Figure 8.** Trends in ozone simulations from CMAQ during 1990-2015 (Unit: ppbv/yr). a) at 8
743 am; b) at 12 pm; c) at 4 pm; d) at 8 pm (all local time). We only show CMAQ grids with
744 statistically significant linear trend in the plots.



745

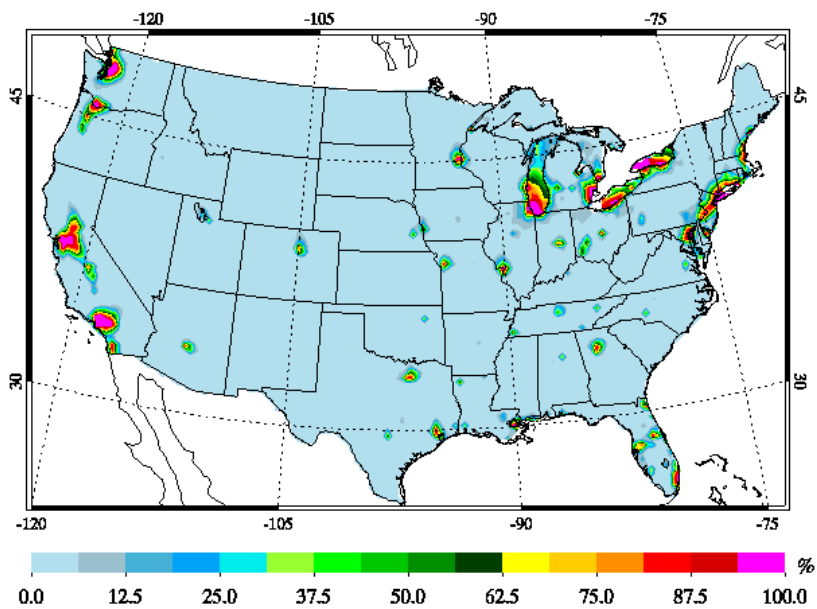
746 **Figure 9.** Trend in O_x ($O_x = O_3 + NO_2$) simulated by CMAQ during 1990-2015. a) at 8 am; b) at
747 12 am; c) at 4 pm; d) at 8 pm (all local time). We only show CMAQ grids with statistically
748 significant linear trend in the plots.



749

750 **Figure 10.** Probability of VOC-sensitive photochemical ozone production (i.e., $O_3/NO_y < 15$) in
751 the CONUS simulated by CMAQ at 2 pm local time in July, a) 1995; b) 2005; and c) 2015

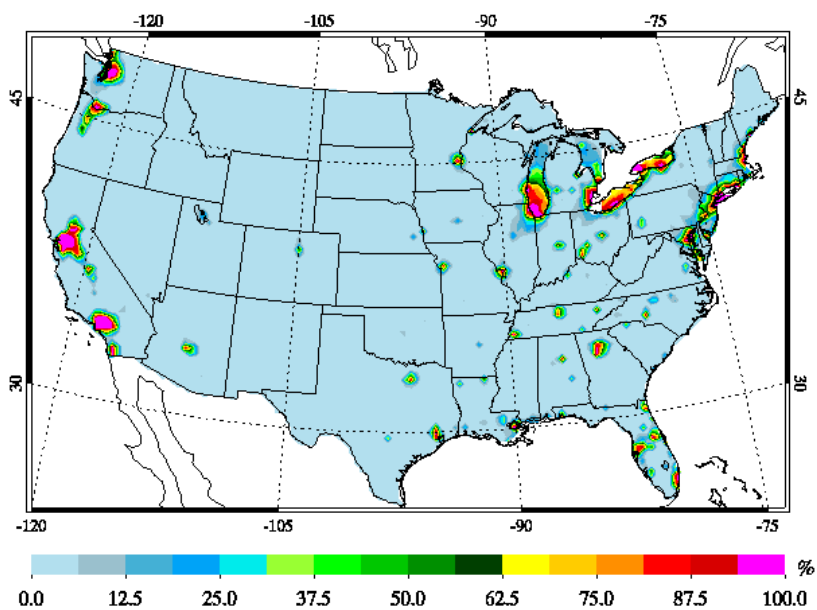
752 a)



753

754

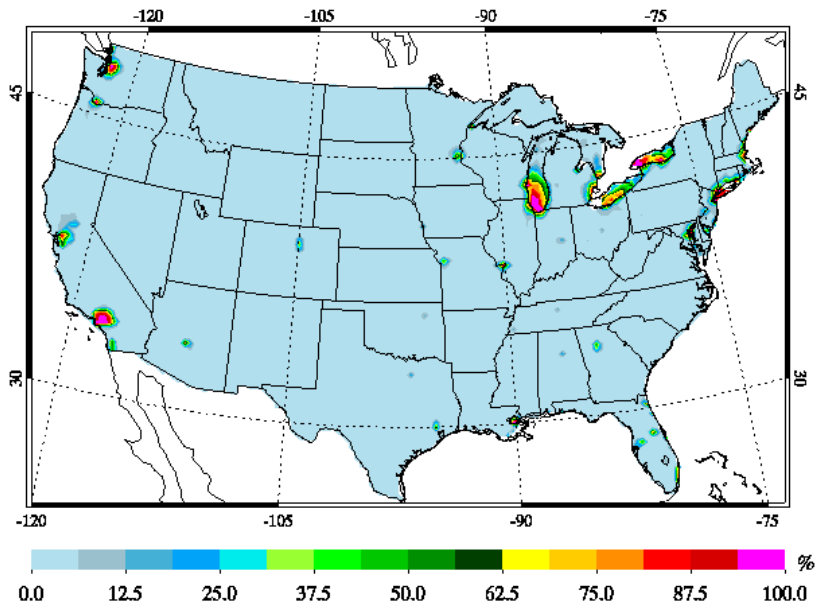
755 b)



756

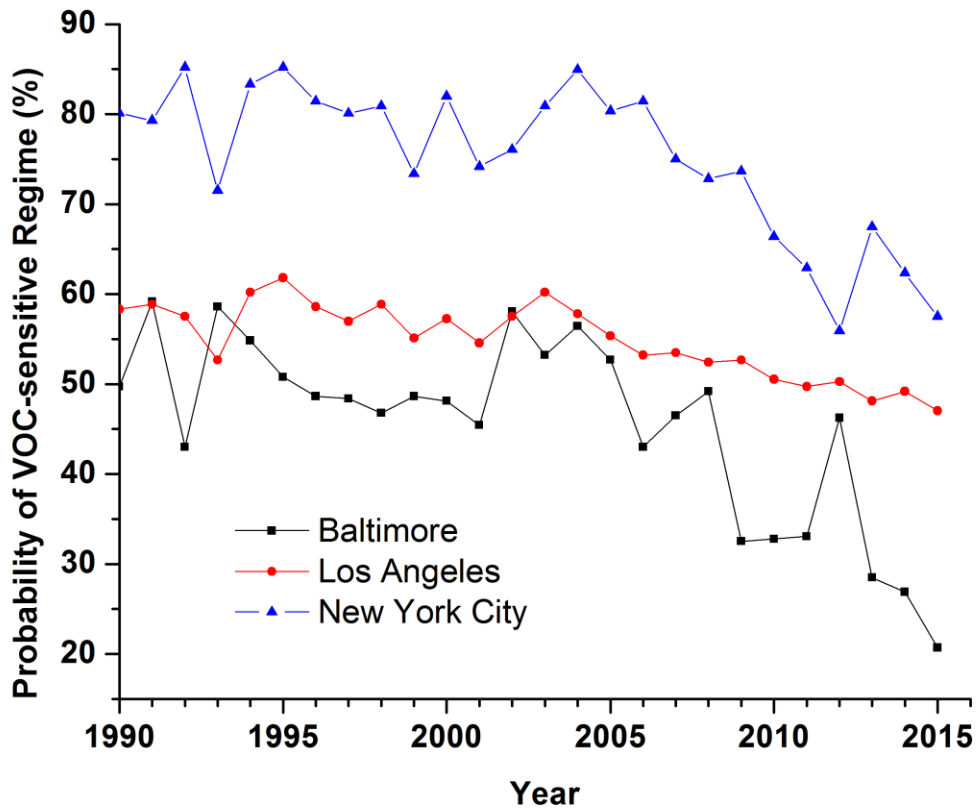
757

758 c)



759

760 **Figure 11.** Long-term trends in probability of VOC-sensitive photochemical production of
761 surface ozone in three major urban areas at 2 pm in July. Probability is calculated using averages
762 of 3×3 grids centered at downtown.



763